

Article (refereed) - postprint

Jutzeler, M.; McPhie, J.; Allen, S. R.. 2014 Facies architecture of a continental, below-wave-base volcanoclastic basin: The Ohanapecosh Formation, Ancestral Cascades arc (Washington, USA). *Geological Society of America Bulletin*, 126 (3-4). 352-376.
[10.1130/B30763.1](https://doi.org/10.1130/B30763.1)

Copyright © 2014 Geological Society of America.

This version available at <http://nora.nerc.ac.uk/506667/>

NERC has developed NORA to enable users to access research outputs wholly or partially funded by NERC. Copyright and other rights for material on this site are retained by the rights owners. Users should read the terms and conditions of use of this material at <http://nora.nerc.ac.uk/policies.html#access>

This document is the author's final manuscript version of the journal article, incorporating any revisions agreed during the peer review process. Some differences between this and the publisher's version remain. You are advised to consult the publisher's version if you wish to cite from this article.

The definitive version is available at <http://www.gsapubs.org/>

Contact NOC NORA team at
publications@noc.soton.ac.uk

1 **Facies architecture of a continental, below-wave-base**
2 **volcaniclastic basin: the Ohanapecosh Formation, Ancestral**
3 **Cascades arc (Washington, USA)**

4

5 **Martin Jutzeler¹, J. McPhie¹, and S. R. Allen¹**6 *¹ Centre of Excellence in Ore Deposits; School of Earth Sciences; University of*7 *Tasmania; Private Bag 79 Hobart, TAS 7001, Australia.*

8

9 First author's current address:

10 *National Oceanographic Centre; European Way, Waterfront Campus; Southampton*11 *SO14 3ZH; United Kingdom*12 *jutzeler@gmail.com*

13

14

15 **ABSTRACT**

16 The >800-m-thick, Oligocene Ohanapecosh Formation records voluminous
17 sedimentation of volcanic clasts in the Ancestral Cascades arc (Washington State,
18 USA). Most volcaniclastic beds are dominated by angular pumice clasts and fiamme
19 of andesitic composition, now entirely devitrified and altered. All beds are laterally
20 continuous and have uniform thickness; fine sandstone and mudstone beds have
21 features typical of low density turbidity currents and suspension settling; erosion
22 surfaces, cross-beds and evidence of bi-directional oscillatory currents (i.e. wave
23 ripples and swaley and hummocky cross-stratification) are almost entirely absent. We
24 infer that the setting was subaqueous and below wave-base.

25 The abundance of angular pumice clasts, crystals and dense volcanic clasts, and
26 extreme thickness of several facies suggest they were derived from magmatic volatile-
27 driven explosive eruptions. The extremely thick beds are ungraded or weakly graded,
28 and lack evidence of hot emplacement, suggesting deposition from subaqueous,
29 water-supported, high-concentration volcanoclastic density currents. Some of the
30 thickest beds contain coarse, rounded dense clasts at their base and are interbedded
31 with accretionary-lapilli-bearing mudstone; these beds are interpreted to be deposits
32 from subaqueous density currents fed by subaerial pyroclastic flows that crossed the
33 shoreline. Shallow basaltic intrusions and mafic volcanic breccia composed of scoria
34 lapilli indicate the presence of intra-basinal scoria cones that may have been partly
35 subaerial.

36 The range in facies in the Ohanapecosh Formation is typical of below-wave-base,
37 continental (lacustrine) basins that form in proximity to active volcanic arcs, and
38 includes eruption-fed and resedimented facies. Extreme instantaneous aggradation
39 rates are related directly to explosive eruptions, and sediment pathways reflect the
40 locations of active volcanoes, in contrast to conventional sedimentation processes
41 acting in non-volcanic environments.

42

43 **INTRODUCTION**

44 The Oligocene Ohanapecosh Formation (Washington State, USA) has been a key
45 reference in the literature on subaqueous explosive volcanism (Fiske, 1963; Fiske et
46 al., 1963). The highly influential work of Fiske (1963) explored general concepts of
47 the nature of explosive eruption-fed subaqueous volcanoclastic density currents – then
48 called “subaqueous pyroclastic flows” – and related them to sources, and transport
49 and depositional processes. Despite the widespread extent of the Ohanapecosh

50 Formation in the central Cascades (>400 km²), and mapping of various sections, the
51 depositional processes and paleo-environment remain debated, in part due to
52 incomplete exposure. This voluminous volcanoclastic succession is basaltic to
53 andesitic in composition, and records the northernmost eruptive activity of the
54 Ancestral Cascades arc (Sherrod and Smith, 2000; du Bray et al., 2006; du Bray and
55 John, 2011).

56 We use facies analysis and the facies architecture of this succession to reassess the
57 eruption styles and paleo-environments of eruption, transport and deposition. We
58 focus on the range of volcanic and sedimentary processes that can reasonably be
59 inferred for voluminous pumice-rich units deposited in a quiet water environment.
60 These processes include subaqueous deposition from subaerial pyroclastic flows that
61 entered water, and subaqueous resedimentation of unconsolidated pumice-rich
62 aggregates. Previous interpretations are re-evaluated.

63 Our facies analysis demonstrates the Ohanapecosh Formation to represent a water-
64 filled depocenter supplied almost entirely by volcanoes. Current understanding of
65 non-volcanic basins (e.g. Johnson and Baldwin, 1996; Stow et al., 1996) cannot be
66 applied directly to basins supplied by active volcanoes, because particle types, particle
67 supply rates, transport and deposition processes, facies (especially bed thickness) and
68 aggradation rates differ substantially. Using evidence from the Ohanapecosh
69 Formation, we discuss the facies characteristics of strongly volcanic-influenced, basin
70 successions, and how they differ from non-volcanic basins.

71

72 **Definitions and methods**

73 The bed thickness nomenclature follows Ingram (1954), and “extremely thick” is
74 added for beds >10 m thick. “Breccia” is used as a non-genetic term to describe any

75 clastic facies composed of angular clasts coarser than 2 mm (Fisher, 1961b); the term
76 “matrix” is used broadly for interstitial clasts <2 mm.

77 Most components of the Ohanapecosh Formation are volcanic, and we follow the
78 nomenclature of McPhie et al. (1993) to describe these rocks. In this paper, volcanic
79 clast-rich rocks are grouped into the broad term “volcaniclastic”; facies generated by
80 explosive eruptions are called “pyroclastic”. “Pumice” is used for highly vesicular
81 (>60 vol.%) volcanic fragments that are intermediate to felsic in composition,
82 whereas “scoria” clasts are less vesicular (<60 vol.%) and mafic in composition.
83 Aligned lenticular clasts are called “fiamme” (Bull and McPhie, 2007) and most
84 appear to have been pumice clasts that compacted during diagenesis, partly or fully
85 losing their initial porosity.

86 U/Pb analyses on zircons by LA-ICP-MS were performed on an Agilent 7500cs
87 quadrupole ICPMS with a 193 nm Coherent Ar-F gas laser and the Resonetics M50
88 ablation cell at the University of Tasmania (Australia). Rocks were crushed in a Cr-
89 steel ring mill to a grain size <400 microns; zircons were paned, separated from
90 magnetic heavy minerals and hand-picked under the microscope. The selected zircon
91 crystals were glued into epoxy and finally polished and cleaned (electronic suppl.).

92

93 **GEOLOGICAL SETTING OF THE OHANAPECOSH FORMATION**

94 **Volcanism and tectonic setting of the Ancestral Cascades arc**

95 Subduction of the Pacific plate under the North American plate began in the Paleozoic
96 era and is still continuing today (Dickinson, 2009). During the Cenozoic, the
97 extremely long (>1,250 km) Ancestral Cascades arc developed on the Paleozoic and
98 Mesozoic continental terranes of western North America. Uncertainties regarding the
99 magmatism of the Ancestral Cascades arc (45-4 Ma; du Bray and John, 2011), and the

100 early Cenozoic history of southern Washington are partly due to loss of the geological
101 record by erosion in response to regional uplift of the northern Cascades (e.g.
102 McBirney, 1978; Hammond, 1979; Reiners et al., 2002), and burial under Miocene
103 and Quaternary volcanoes (Schuster, 2005; Hildreth, 2007).

104 From the Eocene to the middle Oligocene, regional extension and transtension
105 affected the northwestern part of the North American continent (Frizzell et al., 1984;
106 Tabor et al., 1984; Johnson, 1985; Tabor et al., 2000). In southern Washington, major
107 transcurrent faults offset the pre-Tertiary continental basement, in response to oblique
108 subduction beneath the North American plate (Bonini et al., 1974; Johnson, 1984;
109 Johnson, 1985; Armstrong and Ward, 1991; Blakely et al., 2002). From 57 to 43 Ma
110 (Cheney and Hayman, 2009), these faults promoted the formation of separate basins
111 that have distinct sedimentation and deformation histories (Johnson, 1984; Johnson,
112 1985). The fills of these basins comprise the middle to late Eocene Puget Group, and
113 Renton, Spiketon and Naches formations, which are partially conformably overlain by
114 the Ohanapecosh Formation (Tabor et al., 2000). The Ohanapecosh Formation records
115 the northernmost, early magmatism of the Ancestral Cascades arc in southern
116 Washington (Tabor et al., 1984; Johnson, 1985; du Bray and John, 2011).

117 The contact of the Ohanapecosh Formation with the underlying volcanoclastic and
118 siliciclastic Puget Group, and Spiketon and Renton formations is everywhere
119 conformable and commonly gradational (Fiske et al., 1963; Gard, 1968; Simmons et
120 al., 1983; Vance et al., 1987). In contrast, the contact with the underlying Naches
121 Formation is an unconformity (Johnson, 1985; Vance et al., 1987; Tabor et al., 2000).

122 The middle to late Eocene Summit Creek Sandstone (~43 to 37 Ma; Vance et al.,
123 1987) consists of various sandstone units conformably underlying the Ohanapecosh

124 Formation in the areas from the eastern side of White Pass to the Naches River to the
125 east (Ellingson, 1972; Vance et al., 1987; Hammond, 2005).

126

127 **The Ohanapecosh Formation**

128 The mostly volcanoclastic, pumice- and fiamme-rich Ohanapecosh Formation (Fiske
129 et al., 1963) is early to middle Oligocene in age (36 to 28 Ma, mostly dated by fission
130 tracks in zircons; Tabor et al., 2000). However, these dates include samples from a
131 much wider area than the volcanoclastic facies described by Fiske et al. (1963) and
132 this study. In addition, criteria to discern the Ohanapecosh Formation are subtle and
133 its facies are poorly defined amongst the various generations of mappers, therefore it
134 is commonly grouped with other formations into the broad name of Tertiary
135 volcanoclastic units. The Ohanapecosh Formation was thought to be ~3 km thick
136 (Fiske et al., 1963), exposed over >400 km² in an area >700 km² (Schuster, 2005)
137 throughout Mt Rainier National Park and its surroundings, and is the basement upon
138 which Mt Rainier volcano was built (Fig. 1). Coherent facies possibly related to the
139 Ohanapecosh Formation occur at a few places (Fiske et al., 1963; Wise, 1970;
140 Swanson, 1996; Swanson et al., 1997; Hammond, 2011 unpubl. data), and numerous
141 younger dykes intrude the formation (Fiske et al., 1963).

142 The Ohanapecosh Formation *sensu lato* has been recognized from the Snoqualmie
143 area (north) to Columbia River Gorge (south to Mt St Helens and Mt Adams), and
144 from Mt Rainier and Lake Tapps (northwest) to Little Naches River area (east) (Fig.
145 1; e.g. Fisher, 1961a; Fiske et al., 1963; Gard, 1968; Wise, 1970; Ellingson, 1972;
146 Simmons et al., 1983; Frizzell et al., 1984; Evarts et al., 1987; Schasse, 1987; Vance
147 et al., 1987; Smith, 1989; Swanson, 1996; Swanson et al., 1997; Tabor et al., 2000;
148 Hammond, 2005; Schuster, 2005; Hammond, 2011 unpubl. data). Northeast of Mt

149 Rainier, the Ohanapecosh Formation contains sedimentary units derived from a
150 granitic-metamorphic basement, bordering the northern end of the Cascade volcanic
151 arc (Hammond, 1979). A crystalline basement source in eastern Washington and
152 Idaho was suggested by Winters (1984) for feldspathic sandstone that occurs in the
153 Ohanapecosh Formation southeast of Packwood.

154 In the Mt Rainier National Park area, the Ohanapecosh Formation is overlain with an
155 unconformable contact by the Oligocene (25-27 Ma) Stevens Ridge Member, which is
156 the lower part of the Fifes Peak Formation (Vance et al., 1987; Tabor et al., 2000;
157 Hammond, 2011 unpubl. data). This member is composed of multiple 5- to >100-m-
158 thick quartz-bearing rhyolitic ignimbrites, whereas the Fifes Peak Formation is
159 dominated by basaltic and andesitic lavas (Fiske et al., 1963). At Backbone Ridge,
160 southeast of Mt Rainier (Fig. 2), the top of the Ohanapecosh Formation is eroded, and
161 clasts of the Ohanapecosh Formation and tree trunks occur in the base of the lowest
162 ignimbrite of the Stevens Ridge Member (Fiske et al., 1963). In the Mt Rainier
163 National Park, the Stevens Ridge Member was originally defined as a formation by
164 Fiske et al. (1963). However, Tabor et al. (2000) found a gradational boundary
165 between it and the overlying Fifes Peak Formation, and consequently re-defined the
166 Stevens Ridge Formation as a Member of the Fifes Peak Formation. The Fifes Peak
167 Formation covers large areas around Mt Rainier, at Fifes Peak and Tieton (Warren,
168 1941; Fiske et al., 1963; Swanson, 1965, 1966, 1978; Schasse, 1987; Vance et al.,
169 1987; Tabor et al., 2000; Hammond, 2005, 2011 unpubl. data). In southern
170 Washington, the Ohanapecosh Formation is unconformably overlain by the early
171 Miocene Eagle Creek Formation (Wise, 1970), composed of very poorly sorted
172 conglomerate containing pumice fragments, thin-bedded sandstone and pebble
173 conglomerate, and paleosols. These Tertiary formations are mostly covered by thick

174 lavas and volcanoclastic aprons of the modern Cascades arc volcanoes (Mt Rainier,
175 Goat Rocks, Mt Adams, Indian Heaven and Mt St Helens; Fig. 1; Crandell, 1976;
176 Hildreth, 2007).

177

178 **Previous work on facies of the Ohanapecosh Formation**

179 The volcanoclastic facies of the Ohanapecosh Formation in the Mt Rainier area were
180 studied extensively by Fiske (1963) and Fiske et al. (1963, 1964). Various processes
181 and origins have been proposed (Fiske, 1963; Fiske et al., 1963; Winters, 1984; Stine,
182 1987; Vance et al., 1987; Swanson, 1996; Swanson et al., 1997). The formation is
183 mainly composed of andesitic and dacitic volcanoclastic facies; minor lavas, “arkose”
184 and “sandstone” are present locally (Wise, 1970; Winters, 1984; Stine, 1987; Vance et
185 al., 1987). The main volcanic clasts consist of pumice, crystals and dense andesite.
186 Broken and unbroken accretionary lapilli are common in a few facies. Fossils of
187 wood, leaves and poorly preserved benthic shells (“ostracods, gastropods, and perhaps
188 even Foraminifera”; Fiske, 1963) are locally present, but not diagnostic of a marine
189 versus lacustrine environment.

190 The “thick” beds (Fiske, 1963) are well defined and laterally extensive (>hundreds of
191 m), and 3 to 60 m thick (average thickness of 10 m). No welding textures or columnar
192 joints were documented. The “thin” beds (Fiske, 1963) are well defined, laterally
193 extensive over tens of meters, commonly normally graded, and mostly 50-60 cm
194 thick. Some “thin” beds are internally stratified, but sole marks, slump structures and
195 cross laminae are uncommon. Bed pinch-out structures were documented locally
196 southeast of Packwood (Winters, 1984; Stine, 1987). No major faults were identified
197 in previous studies of the Ohanapecosh Formation.

198 Fiske (1963), followed by Wise (1970), proposed that most of the formation was
199 erupted and emplaced subaqueously, in quiet water such as a lake or sheltered
200 embayment of the sea, thus representing the depocenter of underwater volcanoes. The
201 quiet subaqueous depositional setting was inferred on the basis of: the laterally
202 extensive, uniform-thickness bed geometry, internal grading, and the complete
203 absence of unconformities, erosion surfaces and large-scale cross beds. The absence
204 of typically marine fossils suggested a lacustrine rather than marine environment.
205 However, more recent interpretations have assumed - on the basis of weak or
206 incorrect evidence - a subaerial environment of deposition, such as a fluvial and
207 alluvial apron in which lakes were minor, shallow and temporary (Frizzell et al.,
208 1984; Winters, 1984; Stine, 1987; Vance et al., 1987; Swanson, 1996; Swanson et al.,
209 1997; Tabor et al., 2000).

210 The Ohanapecosh Formation is intruded by numerous silicic dykes and sills that are
211 related to the Miocene Tatoosh and Snoqualmie plutons (Fiske et al., 1963; Johnson,
212 1985; Tabor et al., 2000). The dykes are commonly <10 m wide. The Ohanapecosh
213 Formation is locally altered at contacts with the largest sills (>>10 m thick). The
214 formation is well indurated and has a secondary mineral assemblage consistent with
215 low-grade regional metamorphism (zeolite facies). All original glass and most original
216 ferromagnesian and plagioclase phenocrysts have been replaced by secondary
217 minerals. The alteration has been attributed to higher temperature and pressure
218 associated with deep burial and contact metamorphism from intrusions (Fiske et al.,
219 1963).

220

221 **INTERNAL STRATIGRAPHY OF THE OHANAPECOSH FORMATION**

222 In the studied area (Fig. 2), the Ohanapecosh Formation records deposition of almost
223 exclusively volcanoclastic facies. This study subdivides the Ohanapecosh Formation
224 into three main associations that each consists of similar volcanoclastic facies: the
225 Chinook Pass association, the White Pass association and the Johnson Creek
226 association.

227 The Chinook Pass association comprises >350-m-thick volcanoclastic sequences
228 exposed at Cayuse and Chinook Passes and at Cougar Lake (Fig. 3; electronic suppl.).
229 The total thickness of the association is unknown. The Chinook Pass association is
230 characterized by pale green, extremely thick, pumice and fiamme-rich beds of
231 intermediate composition, interbedded with multiple, laterally continuous, thin to
232 thick beds that have similar aspects.

233 The White Pass association is >800 m thick and exposed in the road cuts of White
234 Pass and Backbone Ridge, as well as on the slope from near the Ohanapecosh
235 Campground up to the Backbone Ridge road (Fig. 4; electronic suppl.). The chiefly
236 volcanoclastic White Pass association consists of dark to pale green, thin to extremely
237 thick, pumice- and fiamme-rich beds of mafic and intermediate composition. A mafic
238 component is common, whereas it has not been found in the other two associations of
239 the formation. Thin to thick, fine sandstone and mudstone beds are common.

240 The Johnson Creek association is exposed in scattered road outcrops to the southeast
241 of Packwood (electronic suppl.). The dark green volcanoclastic facies are mostly
242 similar to those in the Ohanapecosh Campground and Backbone Ridge sections
243 (White Pass association), but beds are thinner and show rare cross-laminae and
244 channel-like features. Rare fine grained siliciclastic facies have been reported
245 (Winters, 1984; Stine, 1987).

246

247 **Ohanapecosh Fault**

248 In the White Pass section at the bottom of Ohanapecosh River Valley, two units are
249 used as stratigraphic markers (Fig. 4): an extremely thick (>15 m) bed of red fiamme
250 breccia (unit 143, White Pass section) and a white, 5-m-thick, quartz-rich, matrix-
251 supported volcanic breccia (unit 147, White Pass section). The red fiamme breccia
252 (unit 143) probably correlates with the red fiamme breccia of the Stevens Ridge
253 Member of the Fifes Peak Formation outside the logged area at Backbone Ridge (Fig.
254 4). At the base of White Pass (bed 147, top of the White Pass section), after more than
255 200 m of intervening hidden exposures from bed 143, there is a poorly exposed,
256 white, 5-m-thick bed of quartz-rich, fine ignimbrite that is also attributed to the
257 Stevens Ridge Member. This outcrop of the Stevens Ridge Member and numerous
258 beds higher in the stratigraphy are not shown on any geological maps (Fiske et al.,
259 1963; Schuster, 2005; Hammond, 2011 unpubl. data).

260 On the basis of stratigraphic correlations in the Stevens Ridge Member and the White
261 Pass association (Fig. 4), we infer that a major north-south fault separates the White
262 Pass and Backbone Ridge sections. This fault follows the Ohanapecosh River Valley
263 and is here named the Ohanapecosh Fault (Fig. 4). Its exact location and dip are
264 unknown, but it doubles ~500 m of stratigraphy. The Ohanapecosh Fault accounts for
265 repetition of the red fiamme breccia and quartz-rich fine ignimbrite in the Stevens
266 Ridge Member (Fifes Peak Formation; Fig. 4). On the basis of the White Pass and
267 Backbone Ridge sections, Fiske et al. (1963) proposed a thickness of ~3 km for the
268 entire Ohanapecosh Formation. The fault repetition proposed here decreases the
269 maximum thickness of the formation to >800 m (Fig. 4), because the Ohanapecosh
270 Fault increases the apparent thickness of the White Pass association between White
271 Pass and Backbone Ridge (Fig. 4; electronic suppl.).

272

273 **New U/Pb in zircon dates**

274 Zircons in the lowermost and uppermost beds of the White Pass association have been
275 dated at 31.9 ± 1.4 Ma and 25.94 ± 0.31 Ma, respectively (Fig. 4; electronic suppl.).
276 U/Pb analyses of zircons by LA-ICP-MS of a pumice-rich bed in the Cayuse Pass
277 section gave an age of 29.69 ± 0.68 Ma (Fig. 3; electronic suppl.). These dates restrict
278 the Ohanapecosh Formation to a time interval of ~6 million years, and to be overall
279 younger than previously thought (Vance et al., 1987; Tabor et al., 2000). However,
280 these former studies used samples from a wider area, and a very broadly defined
281 Ohanapecosh Formation. In addition, former ages are essentially derived from fission
282 tracks on zircons, which is a much less accurate technique than the U/Pb by LA-ICP-
283 MS analyses reported here. Method accuracy may explain why the age of the
284 uppermost bed in the Ohanapecosh Formation (this study) is younger than the
285 published fission track age of the overlying Stevens Ridge Member from the Fifes
286 Peak Formation (Vance et al., 1987).

287

288 **COMPONENTS OF THE OHANAPECOSH FORMATION**

289 A dominant intermediate composition of the fiamme, pumice and dense clasts is
290 suggested by abundant plagioclase and minor ferromagnesian phenocrysts. A minor
291 part of the succession is mafic in composition (probably basaltic) and characterized by
292 abundant ferromagnesian and rare feldspar phenocrysts in scoria and dense clasts.
293 Pumice clasts and fiamme (Table 1) are ubiquitous throughout the Ohanapecosh
294 Formation. Fiamme have their long axes oriented parallel to bedding, and they are
295 considered to be former pumice clasts, now compacted. Scoria clasts are present in the
296 White Pass association. Numerous types of dense clasts occur in the Ohanapecosh

297 Formation. The dense clasts are rich in feldspar and ferromagnesian crystals, but lack
298 quartz, which reflects their mafic to intermediate compositions. The dense clasts are
299 aphyric to moderately porphyritic and variably altered. The matrix (<2 mm) now
300 includes crystal fragments (partly to fully altered, mostly feldspar, with minor
301 ferromagnesian minerals). Apart from crystals, matrix is similar in color and texture
302 to the preserved clasts, which strongly suggests that the original components were all
303 volcanic, and had the same bulk composition. Rim-type accretionary and armored
304 lapilli (Schumacher and Schmincke, 1991) were found in a few very thin beds, and
305 can reach 20 mm across. They are absent in the thick to extremely thick beds. Plant
306 fossils and casts of leaves and silicified tree fragments were found at various places,
307 but in minor quantities.

308

309 **FACIES IN THE OHANAPECOSH FORMATION**

310 The Ohanapecosh Formation is composed of 13 major facies, most of them being
311 volcanoclastic and composed entirely of volcanic clasts. The volcanoclastic facies were
312 distinguished on the basis of bed thickness, grading, componentry, grain size and
313 composition. A full description of the facies in the Ohanapecosh Formation is
314 presented in Table 2, and additional field data and complete logs are added as an
315 electronic supplement. The grain size distribution of selected facies was calculated by
316 image analysis and functional stereology (Jutzeler et al., 2012), and will be presented
317 in a further study.

318 Coarse-grained, extremely thick facies occur everywhere in the Ohanapecosh
319 Formation, and make a large part of the Chinook Pass and White Pass associations,
320 where they are interbedded with thinner and finer grained facies. Most of the volume
321 of the Chinook Pass association consists of tabular and laterally continuous, extremely

322 thick beds (up to >40 m) of normally graded fiamme-dense clast breccia (facies 1;
323 Fig. 5), normally graded dense clast-fiamme breccia (facies 2; Fig. 6), normally
324 graded fiamme breccia (facies 3; Fig. 7) and reversely graded fiamme breccia (facies
325 4; Fig. 8), which are mostly composed of fiamme and pumice clasts, crystal fragments
326 and dense clasts; some facies have a basal sub-facies rich in coarse, dense, angular to
327 sub-rounded volcanic clasts. Rare polymictic breccia-conglomerate (facies 7) occurs
328 in the White Pass section.

329 In the White Pass association, the graded or massive volcanic breccia (facies 5; Fig. 9)
330 and massive volcanic breccia (facies 6; Fig. 10) are very thick to extremely thick,
331 laterally continuous, clast- or matrix-supported, and consist of variable amounts of
332 fiamme, pumice clasts, dense clasts, and crystal fragments. In the Chinook Pass
333 association, an unusual very thick (>3 m) succession of reversely to normally graded
334 pumice breccia (facies 8; Fig. 11) occurs. It is extensive over >100 m and composed
335 of six main beds of pumice breccia that are intercalated with tens of beds of
336 mudstone.

337 Most of the very thin to medium thickness beds in the Ohanapecosh Formation are
338 fine sandstone and mudstone (facies 9; Fig. 12). They occur as m-thick groups, are
339 laterally continuous, uniform in thickness, lack cross-bedded structures and
340 commonly contain wood and accretionary lapilli. They are interbedded with the
341 thicker facies. Voluminous successions of basaltic scoria breccia (facies 11; Fig. 13)
342 occur in the White Pass association, and can be associated with vesicular basalt
343 (facies 12), which is rarely found in the Chinook Pass association. Other minor facies
344 include normally graded dense clast breccia to fiamme breccia (facies 10), flow-
345 banded dacite (facies 13), thin to very thick beds of relatively well-sorted, massive

346 mafic sandstone (facies 14), fine, dense clast volcanic breccia (facies 15), and thinly
347 to thickly bedded, normally or reversely graded fiamme mudstone (facies 16).

348

349 **INTERPRETATION AND DISCUSSION**

350 **Origins of clasts in the Ohanapecosh Formation**

351 The high abundance of relatively fine (mostly <10 cm) pumice clasts and fiamme, and
352 crystal fragments in most volcanoclastic facies (Table 1) strongly suggests that these
353 components were produced by explosive eruptions and are thus considered to be
354 pyroclasts. Free broken crystals are interpreted as pyroclasts derived from the same
355 magmas as the pumice clasts and fiamme (Table 1). Scoria clasts are the most
356 abundant components in the basaltic scoria breccia (facies 11) and massive mafic
357 sandstone (facies 14), and are also considered to be pyroclasts. Most dense clasts of
358 the Ohanapecosh Formation contain microlites and phenocrysts that attest to their
359 volcanic origin (Table 1) and have intermediate to mafic compositions. Angular dense
360 clasts that occur with abundant pumice clasts or fiamme are possibly pyroclasts. The
361 origins of sub-angular to rounded dense volcanic clasts cannot be resolved because
362 these clasts were abraded prior to and/or during final deposition. The matrix other
363 than crystals is interpreted to be mostly made of fine, originally glassy pyroclasts.
364 Rare beds of dark grayish brown fine sandstone to mudstone (facies 9) that contain
365 wood chips and leaves are probably partly derived from decay of organic components.
366 A few beds of fine sandstone to mudstone (facies 9) in the Johnson Creek association
367 contain abundant non-volcanic feldspar crystals that reflect continental erosion
368 (Winters, 1984).

369

370 **Depositional setting**

371 Poorly preserved fossils "ostracods, gastropods, and perhaps even Foraminifera"
372 described by Fiske et al. (1963) indicate a subaqueous depositional setting for the
373 Ohanapecosh Formation. In addition, the Ohanapecosh Formation includes several
374 very thinly to thickly bedded facies (facies 9, 14, 15) in which beds are planar and
375 laterally continuous, and that lack cross-stratification, erosional surfaces or paleosols.
376 The overall absence of cross-beds, erosional surfaces and paleosols precludes a
377 subaerial to shallow water setting. Most clasts - including pumice - in the
378 Ohanapecosh Formation are angular, which suggests minimum residence in a
379 subaerial or shoreline environment. We agree with Fiske (1963) that these bed
380 characteristics strongly constrain the depositional setting of most of the formation to
381 below wave base (Fig. 14).

382 The Ohanapecosh Formation was probably deposited in a deep lake, or a protected sea
383 embayment because of its setting close to the continental margin (e.g. McBirney,
384 1978; Johnson, 1985; Dickinson, 2009). The relatively common occurrence of wood
385 chips and leaves in the very thin to thickly bedded facies (facies 8, 9 and 16; Table 1)
386 indicates proximity to land. Lakes are likely to produce scarce carbonaceous facies
387 (Platt and Wright, 1991), have shores with gentler gradients, and wave action is much
388 weaker than in conventional marine settings, reducing coastal erosion and limiting the
389 abundance of well-rounded clasts (e.g. Manville, 2001). Lacustrine environments in
390 active tectonic areas, such as an intra-continental rift, can be deep (i.e. >500 m) and
391 subside rapidly so that subsidence compensates for the high accumulation rates of
392 volcanoclastic facies (e.g. Baltzer, 1991; Gaylord et al., 2001). The lack of facies
393 indicative of shoreline processes, such as coarse conglomerate, well sorted pebbly
394 sandstone, cross-bedded sandstone, evidence of bi-directional oscillatory currents (i.e.
395 wave ripples and swaley and hummocky cross-stratification), mega-breccia from

396 large-scale failure events, and abundant coastal shell fragments (e.g. Busby-Spera,
397 1985; White and Busby-Spera, 1987; Busby-Spera, 1988; Allen, 2004b; Allen et al.,
398 2007) precludes a volcanoclastic apron environment. We infer that the Ohanapecosh
399 Formation accumulated on a quiet, below-wave-base, very low-gradient slope. The
400 presence of accretionary lapilli in fine sandstone to mudstone (facies 8) is not an
401 indicator of the depositional environment, as they can be robust enough to withstand
402 sedimentation and resedimentation in water (e.g. Boulter, 1987).

403 The upper part of the Ohanapecosh Formation is poorly exposed and the presence or
404 the absence of the planar thinly bedded facies, partial indicators of a subaqueous
405 environment, is unknown. The overlying Fifes Peak Formation was deposited
406 subaerially (Fiske et al., 1963), after an episode of erosion and deformation (Fiske et
407 al., 1963; Hammond, 2011 unpubl. data). It is possible that a shallow water or
408 subaerial setting existed during the last stage of deposition of the Ohanapecosh
409 Formation. However, the volume of potentially shallow to subaerial facies is minor
410 compared to the total thickness and extent of the Ohanapecosh Formation.

411

412 **Transport and depositional processes**

413 The lithofacies characteristics suggest that most of very thick to extremely thick
414 clastic facies were produced by high concentration, subaqueous volcanoclastic density
415 currents (Fig. 14, Table 3). In contrast, most very thin to thick beds show better
416 sorting and grading, consistent with deposition from low-concentration density
417 currents and vertical settling from suspension, and are discussed separately below.
418 However, lithofacies analysis in the Ohanapecosh Formation remains difficult
419 because the finest (<2 mm) clasts were destroyed during diagenesis, preventing
420 description of the total grain size distribution.

421

422 *Very thick to extremely thick beds*

423 Most facies of the Ohanapecosh Formation consist of very thick to extremely thick
424 tabular beds with sharp bases that are distinctly graded or massive, and are typical of
425 deposits from high-concentration density currents in general (Lowe, 1982; Mulder and
426 Alexander, 2001; Kokelaar et al., 2007; Piper and Normark, 2009; Sumner et al.,
427 2009; Talling et al., 2012). Such currents can have hot volcanic gas (pyroclastic flows
428 *sensu stricto*) or water as the interstitial fluid. Although composed primarily of
429 pyroclasts, all facies in the Ohanapecosh Formation lack textures related to hot state
430 deposition, such as welding, columnar joints and gas segregation pipes (Cas and
431 Wright, 1991). Also, pumice clasts are typically angular and indicate that clast-to-
432 clast interaction was more limited than is typical of pyroclastic flow transport (e.g.
433 Dufek and Manga, 2008; Manga et al., 2011). Further, the internal textures and
434 organization of the very thick to extremely thick beds are uniform everywhere in the
435 >400 km² area of exposure, indicating that throughout this area, the transport and
436 depositional processes were also uniform. Therefore, the density currents must have
437 propagated for several to tens of km in the below-wave-base setting. There are no
438 examples known of laterally extensive subaqueous pyroclastic flow deposits *sensu*
439 *stricto*, and theoretical arguments imply that gas-supported phases under water should
440 be replaced quickly by water, by condensation of the gas phase during cooling
441 (Legros and Druitt, 2000; Freundt, 2003; Head and Wilson, 2003; Dufek et al., 2007;
442 Allen et al., 2008). Notable exceptions may include very proximal, submarine inner-
443 caldera environment (Busby-Spera, 1986) and where subaerial pyroclastic flows
444 rather push than enter a water body (Legros and Druitt, 2000) where flat shore occur.

445 On this basis, we infer that the Ohanapecosh Formation volcanoclastic density currents
446 were water-supported, rather than hot gas-supported.

447 The term “subaqueous volcanoclastic density current” is used for the density currents
448 that produced the very thick to extremely thick facies in the Ohanapecosh Formation
449 (Table 3); the term is intended to imply that the density currents were water-
450 supported, high concentration and composed of volcanic particles and is inclusive of
451 all the triggering mechanisms (eruption-fed versus resedimentation) and source
452 settings (subaerial versus subaqueous). The apparently abundant matrix and poor
453 sorting in the extremely thick facies suggest deposition from a type of volcanoclastic
454 density current in which the particle concentration was very high and turbulence was
455 suppressed.

456

457 *Very thin to thick beds*

458 Very thin to thick beds in the Ohanapecosh Formation are laterally continuous and
459 have a uniform thickness, which suggests deposition from a combination of
460 suspension settling and low density turbidity currents. Low density pumice clasts and
461 very fine particles can be temporarily suspended in the water column. Settling
462 involves discrete particle fallout and/or vertical density currents, minimal particle
463 interaction and typically produces very good hydraulic sorting (Rubey, 1933;
464 Cashman and Fiske, 1991; Wiesner et al., 1995; Manville et al., 2002; Burgisser and
465 Gardner, 2006). In the reversely to normally graded pumice breccia (facies 8) at
466 Chinook Pass, the lateral continuity of the pumice-dominated beds, presence of
467 mudstone interbeds and the sub-rounded shape of the pumice clasts (Fig. 11; Table 3)
468 suggest that the pumice clasts settled from pumice rafts (Fig. 14a; e.g. White et al.,
469 2001; Manville et al., 2002).

470 Beds of fine sandstone and mudstone (facies 9) in the Ohanapecosh Formation are
471 interpreted to be deposits from low density turbidity currents (turbidity currents *sensu*
472 *stricto*; Bouma, 1962; Lowe, 1982; Shanmugam, 2002) or suspension in the water
473 column (Fig. 14; Table 3). Conventional low density turbidity currents *sensu stricto*
474 are defined by their high degree of turbulence and lack of cohesion; they can transport
475 a relatively low concentration (<10 vol.%) of mostly fine-grained (<2 mm) clasts
476 under water (Lowe, 1982; Mulder and Alexander, 2001; Piper and Normark, 2009)
477 and commonly produce regular successions of relatively thin (up to a few m) beds that
478 are massive or graded (Bouma, 1962; Lowe, 1982; Shanmugam, 2002).

479

480 **Eruption-fed versus resedimented pyroclastic facies**

481 Distinguishing between eruption-fed and resedimentation-driven processes of
482 initiation of subaqueous volcanoclastic density currents is an ongoing challenge
483 (Fisher and Schmincke, 1984; McPhie et al., 1993; White, 2000; White et al., 2003).
484 Piper and Normark (2009) concluded that there is no simple relationship between the
485 characteristics of subaqueous density current deposits and the initiating processes.
486 Subaerial explosive eruptions may generate a wide range of eruption-fed subaqueous
487 facies, including subaqueous volcanoclastic density current deposits and suspension
488 deposits (e.g. Sparks et al., 1980; Yamada, 1984; Whitham and Sparks, 1986;
489 Whitham, 1989; Cas and Wright, 1991; Carey et al., 1996; Mandeville et al., 1996;
490 White et al., 2001; Manville et al., 2002; Freundt, 2003; Dufek et al., 2007). The
491 lower, concentrated part (“basal underflow”) of subaerial pyroclastic flows may be
492 dense enough to enter a body of water and transform into water-supported subaqueous
493 volcanoclastic density current; the much more dilute overriding ash cloud and
494 pyroclastic surges can travel over water for some distance (e.g. White, 2000; Freundt,

495 2003; Edmonds and Herd, 2005; Dufek et al., 2007). Pumice-forming, explosive
496 eruptions can also occur from sea-floor vents, producing density currents underwater
497 (Fiske, 1963; Kokelaar, 1983; Kano, 2003; White et al., 2003; Allen and McPhie,
498 2009). Furthermore, subaqueous volcanoclastic density currents can originate from
499 resedimentation of saturated aggregates (Allen and Freundt, 2006).

500 The presence of pumice clasts in submarine water-supported volcanoclastic density
501 current deposits implies that the pumice clasts were denser than water when entrained
502 in the current. The pumice clasts available for transport in subaqueous volcanoclastic
503 density currents can be: (1) sufficiently hot on contact with water to ingest water
504 immediately and sink (Cas and Wright, 1991; Allen et al., 2008), (2) already
505 sufficiently waterlogged (Allen and Freundt, 2006), and/or (3) low-vesicularity types
506 that are denser than water. Pumice clasts with a vesicularity <60 vol.% will sink
507 because their density is greater than that of water, regardless of the vesicles being gas-
508 or water-filled (Manville et al., 1998; White et al., 2001; Manville et al., 2002). (Cas
509 and Wright, 1991). Pumice clasts of intermediate composition commonly have
510 vesicularities <60 vol.% (e.g. Whitham, 1989; Allen, 2004a).

511 Assessing the source and the transport processes on the basis of deposit characteristics
512 is especially difficult for pyroclast-rich facies in which there is no evidence of hot
513 emplacement (e.g. Cas and Wright, 1991), as in the case for volcanoclastic units in the
514 Ohanapecosh Formation. The characteristics used herein to infer a pumice-forming,
515 explosive eruption-fed origin for volcanoclastic density current deposits include
516 abundant pumice clasts and crystals fragments that reflect a single magma
517 composition, and very thick to extremely thick sedimentation units that reflect large
518 eruption volumes (Table 3). On the other hand, resedimentation events are expected to
519 involve diverse clast compositions, thus generating deposits that are strongly

520 polymictic. Resedimentation processes affect pre-existing unconsolidated deposits,
521 and each resedimentation event is likely to remove only a portion of the pre-existing
522 deposits. Thus, the volumes (and thicknesses) of single beds derived from
523 resedimentation events are predicted to be smaller in comparison to eruption-fed beds,
524 especially in cases involving felsic and intermediate explosive eruptions.

525

526 *Eruption-fed units in the Ohanapecosh Formation*

527 The normally graded fiamme-dense clast breccia (facies 1), normally graded dense
528 clast-fiamme breccia (facies 2), normally graded fiamme breccia (facies 3), reversely
529 graded fiamme breccia (facies 4) and some beds of graded or massive volcanic
530 breccia (facies 5) are all characterized by extreme bed thickness, massive aspect and a
531 high abundance of pyroclasts of similar composition. These facies are interpreted to
532 be explosive eruption-fed products (Fig. 14; Table 3).

533 In the reversely to normally graded pumice breccia (facies 8), pumice clasts are sub-
534 rounded, and dense clasts are absent. The distinctive grading of facies 8 is consistent
535 with saturation grading (Fig. 11). Waterlogging of pumice clasts a few cm in diameter
536 is immediate when the pumice clasts are still hot, whereas it can take up to several
537 months if the pumice clasts are cold and highly vesicular (Whitham and Sparks, 1986;
538 Manville et al., 1998; White et al., 2001; Bryan et al., 2004). Therefore, facies 8 is
539 probably eruption-fed, but the complex grading and presence of mudstone (likely to
540 consist originally of glassy ash) and accretionary lapilli interbeds indicate that the
541 pumice clasts sank progressively in batches from rafts (Fig. 14).

542 In the White Pass section, a succession of upward arching, normally graded and well
543 sorted beds of basaltic scoria breccia (facies 11) that includes impact sags (Fig. 13a;
544 Table 2) is interbedded with fine sandstone and mudstone (facies 9) that contains

545 accretionary lapilli. The succession is interpreted to be the remnant of a scoria cone,
546 probably produced by a combination of strombolian and surtseyan activity (Kokelaar,
547 1986; White, 2001), and most beds are considered to be eruption-fed, or slightly
548 resedimented on the steep slopes of the volcanic cone (Fig. 14c). Units of vesicular
549 basalt (facies 12) beneath the scoria cone facies are probably related to shallow
550 intrusions or small lavas.

551

552 *Resedimented units in the Ohanapecosh Formation*

553 The polymictic breccia-conglomerate (facies 7) is likely to be resedimented, because
554 it contains rounded clasts that were abraded in an above wave-base environment, and
555 occurs in a bed that is only 3 m thick. Some of the beds of basaltic scoria breccia
556 (facies 11) are likely to represent short-distance resedimentation on the scoria cone
557 (Fig. 14). The graded or massive volcanic breccia (facies 5), massive volcanic breccia
558 (facies 6) and some of the beds of fine sandstone and mudstone (facies 9) are not
559 diagnostic of a single initiation process, and can be either eruption-fed or
560 resedimented, and both alternatives probably occur (Fig. 14).

561

562 **Setting of source volcanoes**

563 The abundance of pyroclasts in the Ohanapecosh Formation attests to its origin from
564 explosive eruptions (Table 3). The laterally continuous, very thin to thick beds imply
565 deposition in a subaqueous environment. However, the setting of source vents is
566 difficult to constrain for most facies although both subaerial and subaqueous vents are
567 possible, and may have co-existed; a chiefly subaerial setting of source volcanoes is
568 preferred. The most efficient ways to introduce voluminous pumice and dense clasts
569 to a subaqueous setting are by subaerial pyroclastic flows crossing the shoreline

570 (Whitham, 1989; Cas and Wright, 1991; Allen and Smith, 1994; Kurokawa and
571 Tomita, 1998; Legros and Druitt, 2000; Allen et al., 2003; Freundt, 2003; Allen et al.,
572 2012), or alternatively by subaqueous explosive eruptions (Busby-Spera, 1986; Allen
573 and McPhie, 2009). Subaqueous eruptions are not likely to have been persistent
574 throughout the millions of years of the Ohanapecosh Formation, and known facies
575 derived from subaqueous explosive eruptions (Cas and Wright, 1991; Kano, 2003;
576 Allen et al., 2008; Allen and McPhie, 2009) are not represented in the Ohanapecosh
577 Formation. The vents of intra-basinal subaqueous volcanoes would rapidly reach the
578 water surface, considering the growth of the volcanic edifice and minor wave erosion
579 in a quiet lake environment, filling the basin and producing distinctive above wave-
580 base facies at its top. In addition, the many facies of the Ohanapecosh Formation
581 imply multiple sources, thus many of them would not be positioned in the basin, but
582 at its rim. It is more likely that most of the vents associated with the Chinook Pass
583 association were subaerial, because rare intercalated facies contain rounded clasts
584 resedimented from above wave-base environments (polymictic breccia-conglomerate,
585 unit 58 in the Chinook Pass section; facies 7). Pumice-rich facies interpreted to
586 originate from pumice rafts, and accretionary lapilli occur together in unit 60 of the
587 Chinook Pass section (facies 8; Table 3), both of which imply the existence of a
588 subaerial eruption plume. In addition, the basal dense clast breccia in the three
589 extremely thick, fiamme-rich facies (facies 1–3) include coarse sub-rounded dense
590 clasts that could have been collected at the shoreline, although such rounded clasts
591 may have been previously transported under water from the shore (such as facies 7)
592 and picked-up by the newly arriving density currents. These facies (1, 2, 3, 7, 8) all
593 occur interbedded in the Chinook Pass association, and all other intercalated facies are
594 in conformable contact and contain similar clast types, suggesting a similar source.

595 Hence, the entire Chinook Pass section is most likely to have been chiefly generated
596 by subaerial pyroclastic flows that crossed a shoreline and transformed into water-
597 supported volcanoclastic density currents. In addition, the pumice rafts represented by
598 unit 60 (facies 8) probably formed immediately before or after a climactic eruption
599 represented by extremely thick beds of reversely graded fiamme breccia (facies 4;
600 units 59 and 61, respectively). We infer that the broadly similar, extremely thick beds
601 of the fiamme-rich facies (facies 1–4) in the other associations have the same origin.
602 Some features in facies 1–4 deserve particular consideration. The pumice clasts are
603 distinctly angular and there is abundant matrix (<2 mm), at least in the middle and
604 upper sub-facies. Pumice clasts transported in pyroclastic flows are quickly rounded
605 (e.g. Dufek and Manga, 2008; Manga et al., 2011) so the angular clasts imply that
606 transport by this mode was short. The poor sorting suggests that transport of pumice
607 clasts in water-supported density current was relatively short because in general this
608 transport mode results in relatively good grading and sorting (White, 2000). Thus, the
609 distance between the vents and the deposition site was probably short, and the source
610 volcanoes were nearby. The apparent abundance of matrix in facies 1–4 also suggests
611 that the pyroclastic flows were not very expanded when they crossed the shoreline
612 (e.g. Cas and Wright, 1991).

613

614 **The Ohanapecosh Formation basin**

615 *Chinook Pass association*

616 The Chinook Pass association comprises volcanoclastic facies from one main source,
617 because most clasts have similar mineralogy and composition, and the beds have been
618 deposited by similar types of subaqueous volcanoclastic density currents. Most of the
619 thickness of the Chinook Pass association (~70% of the exposed sections) is

620 dominated by extremely thick, tabular and laterally continuous beds that originated
621 from subaerial pyroclastic flows (normally graded fiamme-dense clast breccia, facies
622 1; normally graded dense clast-fiamme breccia, facies 2; normally graded fiamme
623 breccia, facies 3; reversely graded fiamme breccia, facies 4). Each extremely thick
624 bed in the Chinook Pass association was probably related to a magma eruption
625 volume of 0.1 to $>10 \text{ km}^3$. These extremely thickly bedded facies are interbedded
626 with facies composed of much thinner beds (e.g. facies 5, 9 and 15). Such a transition
627 from single eruption-fed beds to multiple, compositionally similar but much thinner
628 beds may record voluminous deposition from a large-scale explosive eruption,
629 followed by syn- to post-eruptive resedimentation of more proximal, upslope deposits
630 into deeper water (Fig. 15). The latter is preferred for the Chinook Pass association,
631 because most facies in the Chinook Pass association consist of the same coarse
632 components, suggesting that following the main eruptive events, parts of the eruption-
633 fed deposits upslope were resedimented in the Chinook Pass association. The
634 relatively thinly bedded intervals probably also include deposits that are unrelated to
635 eruptions, and instead represent the “background” sedimentation.

636

637 *White Pass association*

638 The White Pass association comprises volcanoclastic facies from at least two main
639 sources. One source produced voluminous and widespread pumiceous volcanoclastic
640 facies of intermediate composition that occur in very thin to extremely thick, planar
641 and laterally continuous beds (graded or massive volcanic breccia, facies 5; massive
642 volcanic breccia, facies 6; fine sandstone and mudstone, facies 9). Whether these
643 source volcanoes were subaqueous, subaerial or both, and whether some beds of the
644 facies are eruption-fed could not be determined from facies characteristics. However,

645 the abundance of beds, most of them polymictic, strongly suggest that many beds are
646 derived from resedimentation, and that resedimentation processes greatly contributed
647 to the filling of the basin. The second source generated small-volume, basaltic, very
648 thinly to thickly bedded volcanoclastic facies (fine sandstone and mudstone, facies 9;
649 massive mafic sandstone, facies 14; basaltic scoria breccia, facies 11). These facies
650 were generated by intrabasinal, weakly explosive, basaltic eruptions and
651 resedimentation, from one or more shallow-water or subaerial vents (Figs 14, 16).

652 In modern subaqueous basins, maximum bed thickness and maximum coarseness
653 occur close to the main transport path and in a medial position relative to the source
654 (e.g. Trofimovs et al., 2006). Distal and lateral equivalents are thinner and finer
655 grained. Strong differences in grain size and average bed thickness that occur between
656 sections in the White Pass association (Fig. 4; Fig. 15) could reflect two settings in
657 relation to the sediment transport path, or intercalation of proximal and distal deposits
658 of two volcanic sources respectively. The White Pass section contains the coarsest and
659 thickest beds of the White Pass association (up to 25 m; massive volcanic breccia,
660 facies 6). This section is interpreted to record deposition centered on the main
661 sediment transport path at a medial position from the source, in a low-gradient basin.

662 In the lower part of the White Pass section, stacks of facies 5 are overlain by stacks of
663 facies 6, which reflects an increase in thickness (electronic suppl.) and coarseness
664 (Fig. 4; electronic suppl.) of the beds. Such a dramatic change may result from
665 progradation (Busby-Spera, 1988), or from different sources and/or pathways of
666 sedimentation. In comparison, beds present in the Ohanapecosh Campground and
667 Backbone Ridge sections are overall thinner and finer grained (fine sandstone and
668 mudstone, facies 9; fine, dense clast volcanic breccia, facies 15; normally or reversely
669 graded fiamme mudstone, facies 16). These sections were probably situated in more

670 distal and/or lateral positions compared to the main sediment transport path recorded
671 in the White Pass section. These facies variations suggest a main broad westward
672 direction of sediment transport in the White Pass association.

673 The two sections of the White Pass association from each side of the Ohanapecosh
674 Fault include multiple beds of basaltic scoria breccia (facies 11; Fig. 13). These beds
675 are interpreted to broadly correlate. The thick sequence of basaltic scoria breccia
676 containing fine sandstone and mudstone (facies 9) with accretionary lapilli and
677 intrusions of vesicular basalt (facies 12) in the White Pass section indicate proximity
678 to a subaerial to shallow water scoria cone, whereas the thinner sequences of basaltic
679 scoria breccia in the Ohanapecosh Campground and Backbone Ridge sections
680 probably formed at a greater distance from the vent(s).

681

682 *Johnson Creek association*

683 The Johnson Creek association consists of very similar facies to the Backbone Ridge
684 section of the White Pass association, and is therefore interpreted in a similar way. It
685 is chiefly composed of thin to very thick beds of pumice fragments of intermediate
686 composition (graded or massive volcanic breccia, facies 5; normally or reversely
687 graded fiamme mudstone, facies 16). These facies probably accumulated in a distal
688 and/or lateral environment with respect to the coarser and thicker facies in the White
689 Pass association. A broadly westward direction of sedimentation was proposed by
690 Winters (1984) on the basis of minor beds of fine sandstone and mudstone containing
691 clasts derived from pre-Tertiary basement rocks.

692

693 *Basin architecture and duration*

694 The Ohanapecosh Formation provides a good example of the complexity possible in
695 subaqueous volcanoclastic basins (Figs 15, 16). The age of the lowermost (31.9 ± 1.4
696 Ma) and uppermost (25.94 ± 0.31 Ma) beds in the White Pass association constrain the
697 >800 m of volcanoclastic sediments to have been sedimented during ~6 million years.
698 An average sedimentation rate of 65-120 m/my can be estimated considering the two
699 beds are separated by 500 m in the stratigraphy (Fig. 4). The three associations are
700 close enough (<10 km) to be part of a single, wide basin. However, the lithofacies of
701 the Chinook Pass association are different from those in the White Pass association
702 and Johnson Creek association. The difference could be explained by supply from
703 different volcanic sources, and/or by the presence of two sub-basins within a larger
704 basin. The poor exposure between the studied sections precludes a better
705 understanding of the stratigraphic relationships between the depocenters.

706

707 *Sources of the Ohanapecosh Formation*

708 The regional extent (>400 km²) and >6 million years in duration of the Ohanapecosh
709 Formation (Tabor et al., 2000; Schuster, 2005; this study), the presence of the
710 remnants of at least one scoria cone in the White Pass association (facies 11, Fig. 13),
711 and the variations in clast mineralogy (Tables 1, 2) all imply that volcanoclastic
712 sediments were supplied from multiple volcanic edifices (Fiske, 1963; Vance et al.,
713 1987; this study). The major eruption centers that fed the Ohanapecosh Formation
714 have not been identified. Lavas or shallow intrusions that could be marking the
715 locations of source vents for the volcanoclastic facies are uncommon and not
716 obviously related to the volcanoclastic facies. Minor lavas within the eastern and
717 northeastern part of the formation (sensu lato) are contemporaneous (Hammond, 2011
718 unpubl. data). Coherent andesite units found in the area southeast of Packwood

719 (Swanson, 1996; Swanson et al., 1997) and at Indian Bar (Fiske et al., 1964) were
720 identified as possible sources of the Ohanapecosh Formation, however nearby
721 volcanoclastic facies could not be directly correlated to these units. The flow-banded
722 dacite (facies 13) at Cougar Lake is probably contemporaneous with the Ohanapecosh
723 Formation, and reflects emplacement of an intrabasinal lava or dome.

724 The Mt Aix caldera, 20 km southeast of Chinook Pass (Fig. 1), is a plausible source of
725 the Ohanapecosh Formation. The age of the caldera-forming eruption (24.7 Ma;
726 Hammond, 2005) is too young compared to the Ohanapecosh Formation, and it
727 produced a rhyolitic ignimbrite (Bumping River tuff). Silicic calderas can be long-
728 lived and commonly form after a period of volcanism involving less evolved
729 (andesitic) magma (e.g. Bailey et al., 1976; Bacon, 1983). Thus, pre-caldera volcanic
730 activity at the vicinity of the Mt Aix caldera could have been a source of the
731 Ohanapecosh Formation. With the exception of the White Pass example, it remains
732 unclear whether or not the mafic intrusions (vesicular basalt, facies 12) were a source
733 of the Ohanapecosh Formation. The White Pass and Chinook Pass associations (Fig.
734 15) comprise facies that reflect filling of the basin primarily during eruptions and the
735 immediate post-eruptive period of resedimentation (e.g. Busby-Spera, 1988; Smith,
736 1991).

737

738 **The Ancestral Cascades arc in Washington**

739 Extending over more than $>400 \text{ km}^2$ in Washington, the Ohanapecosh Formation
740 records an important part of the northern tip of the Ancestral Cascades arc (45–4 Ma,
741 du Bray and John, 2011) during the Oligocene. The depocenter could have formed as
742 a far-field response to the regional extension farther to the northeast during the
743 Eocene (Johnson, 1984; Johnson, 1985; Vance et al., 1987; Cheney and Hayman,

744 2009; Evans, 2010), and thus extend the time and area affected by this regional
745 extension event.

746 The remnants of magmatic activity are more abundant in Washington for the late
747 Oligocene to Miocene period, suggesting a peak of volcanic activity around 25 Ma
748 (e.g. du Bray and John, 2011). However volumetric comparisons should be subject to
749 caution, considering how volcanoclastic deposits are relatively poorly preserved and
750 much less studied in comparison to lavas and intrusions, as exemplified with the few
751 contributions on the Ohanapecosh Formation. Thus, the importance and volume of
752 volcanoclastic deposits are likely to be wrongly minimized (e.g. du Bray et al., 2006).
753 In central Washington, several volcanic centers and intrusions were emplaced after
754 the deposition of the Ohanapecosh Formation, and confirm the continuation of the
755 magmatism in the Ancestral Cascades arc in central Washington. The relationship
756 between the Ohanapecosh Formation and its overlying formations (in particular the
757 Fifes Peak Formation) remains poorly understood and they are likely to be part of
758 different eruptive cycles. Volcanic rocks to the northeast were mostly grouped into the
759 Fifes Peak Formation (Fiske et al., 1963; Tabor et al., 2000; Hammond, 2011 unpubl.
760 data), and important late Oligocene to Miocene volcanic centers include the Mount
761 Aix caldera (late Oligocene), Timberwolf Mountain volcano (late Oligocene), Fifes
762 Peak volcano (Oligocene-Miocene) and Tieton volcano (Late Miocene), and
763 intrusions include the Tatoosh pluton (Late Miocene), Bumping Lake granite
764 (Oligocene) and White River pluton (Miocene) (Fig. 1; Fiske et al., 1963; Swanson,
765 1966; Hammond, 2005, 2011 unpubl. data). The relationship of the Oligocene-
766 Miocene Snoqualmie plutons in central Washington with the Ancestral Cascades arc
767 remains unclear (du Bray and John, 2011).

768 In Washington and Oregon, 45 million years of Ancestral and modern Cascades arc
769 magmatic activity has been concentrated in a relatively narrow segment of continental
770 crust (Sherrod and Smith, 2000; Schuster, 2005) indicating that the volcanic front has
771 remained in more-or-less the same position relative to the subduction zone. This
772 apparent stability could be responsible for the Ohanapecosh basin remaining an active
773 depocenter for ~6 million years, and for the largely intact preservation of the basin
774 fill. This long-lived basin strongly suggests the Ohanapecosh Formation to chiefly
775 record explosive activity and erosion from multiple volcanic centers, principally to the
776 east, north and south of the studied area. In contrast, the southern segment of the
777 Ancestral Cascades arc from Nevada to California migrated westwards in response to
778 slab roll-back (Colgan et al., 2011) throughout the Oligocene, Miocene and Pliocene.
779 Volcaniclastic basins also formed in the southern segment of the arc (Busby, 2012),
780 but they were relatively short lived (e.g. <1.5 million years; Busby et al., 2006),
781 accumulated thicker sediment piles (10 and 4 km during very fast basin subsidence,
782 respectively; Busby et al., 2005; Busby et al., 2006), and were substantially disrupted
783 by fault active during and after filling (Busby and Bassett, 2007). The differences
784 between the two segments of the Ancestral Cascades arc have been attributed to the
785 presence of a long-lived slab tear in the Farallon plate (Colgan et al., 2011).

786

787 **Characteristics of deep subaqueous volcanoclastic basins**

788 The Ohanapecosh Formation lacks shallow water facies, implying sedimentation in a
789 relatively deep lake, or in a basin subsiding at the same rate as filling. In addition, the
790 Ohanapecosh basin had a low gradient, because the succession does not include any
791 slide and slump-related facies. Therefore, the Ohanapecosh Formation had a similar
792 setting to other below-wave-base, deep, quiet basins (e.g. Johnson and Baldwin, 1996;

793 Stow et al., 1996), but it consists of very different and distinctive facies. Deep, quiet,
794 non-volcaniclastic basins comprise turbidites and suspension-settled facies that may
795 relate to sediment dispersal via submarine fans (e.g. Johnson and Baldwin, 1996;
796 Stow et al., 1996; Talling et al., 2012). Single events (flood, landslide, earthquake,
797 etc.) that produce density currents can introduce huge volumes (up to 100 km³) of
798 sediments (Talling et al., 2012). Single turbidites range in thickness of a few cm to
799 ~10 m, depending on their proximity to source, and are typically composed of <2-
800 mm-particles, relatively well sorted and commonly graded (Piper and Normark, 2009;
801 Talling et al., 2012).

802 Non-volcanic detritus in the Ohanapecosh Formation (i.e. organic matter and fine
803 sandstone and mudstone of continental origin; part of facies 9) is minimal (< a few
804 vol.%), and implies that the depocenter was almost exclusively supplied by volcanic
805 processes. Andesitic explosive eruptions were the principal supplier of sediment, and
806 this sediment was delivered by means of eruption-fed subaqueous volcanoclastic
807 density currents, and by re-sedimentation events. Each extremely thick bed was
808 probably related to a magma volume of 0.1–10 km³ erupted more-or-less
809 instantaneously. From our zircons ages, the average sedimentation rate in the White
810 Pass association is 65–120 m/my, which is comparable to accumulation rates at 30 km
811 offshore Montserrat island (90 m/my; Expedition 340 Scientists, 2012) and in some
812 conventional siliciclastic environments (e.g. Sadler, 1981). Eruptions and syn-eruptive
813 re-sedimentation events are rapid, producing extreme instantaneous aggradation rates
814 (m to tens of m per hour/year). Single subaqueous volcanoclastic density currents must
815 be more voluminous and/or prolonged and more concentrated than single turbidity
816 currents because their deposits are much thicker, less well sorted, less well graded and

817 in most cases, coarser than conventional turbidites. Wide variations in pyroclast
818 density, size and shape produce facies that cannot be generated by other mechanisms.
819 In active volcanic arc settings, the eruption-fed sediment supply is controlled by
820 eruption frequency, style and magnitude. Sediment dispersal pathways are related to
821 the locations of active volcanoes. In addition, explosive volcanic eruptions disperse
822 large volumes of pyroclasts over wide areas, eliminating any sediment from other
823 sources. In some cases, pyroclasts are introduced independently of established surface
824 pathways, such as by settling of pumice from pumice rafts, or settling of accretionary
825 lapilli and ash from the atmosphere to the water column over large areas (facies 8 and
826 9).

827

828 **CONCLUSIONS**

829 The >400 km² Ohanapecosh Formation (Washington State, USA) is an Oligocene
830 volcanoclastic succession generated by volcanism in the Ancestral Cascades arc. The
831 formation is mainly composed of andesitic volcanoclastic facies and was deposited
832 over ~6 million years. The thickness of the formation in the studied area is >800 m,
833 and part of the succession has been repeated by an inferred fault in the Ohanapecosh
834 River Valley. Three associations have been defined on the basis of lithofacies
835 characteristics and area of distribution. Multiple sources, eruption styles, and transport
836 and depositional processes are necessary to explain the extent and diversity of the
837 volcanoclastic lithofacies. However, the depositional setting remained subaqueous and
838 below wave-base, and the environment of deposition was low-energy, such as within
839 a continental basin. The lack of lenticular conglomerate and well-sorted cross-bedded
840 sandstone typical of shoreline settings suggests the original basin was larger than the
841 preserved remnants. The most abundant facies (by volume) are extremely thick (up to

842 50 m), internally massive or graded, and composed of andesitic pyroclasts. They were
843 deposited from eruption-fed, water-supported, subaqueous volcanoclastic density
844 currents generated by pyroclastic flows that crossed the shoreline.

845 Below-wave-base deposition in basins associated with active subaerial volcanoes
846 differs from that of non-volcanic basins. The supply of sediments is controlled by the
847 frequency, style and magnitude volcanic eruptions, and sediment pathways are
848 influenced by the locations of active volcanoes. The instantaneous accumulation rate
849 of deposits from single explosive eruption-fed events in a volcanic arc basin is likely
850 to be much higher than in a non-volcanic environment, even though the average
851 accumulation rate may be similar or lower. The longevity and overall good
852 preservation of the Ohanapecosh basin possibly reflects the relative stability of the
853 northern Cascades arc compared with the extension-affected southern Cascades arc.

854

855 **ACKNOWLEDGMENTS**

856 The research is part of the PhD thesis of M. Jutzeler and was funded by ARC-CODES
857 grants to the authors. We warmly thank R. Fiske and P.-E. Hammond for helpful
858 discussions in the field and during the study. V. Manville, C. Busby, R. Fiske and R.
859 Cas are acknowledged for their reviews of previous manuscripts. Part of this study
860 was supported by USGS-funded Jack Kleinman 2009 grant.

861

862 **FIGURES**

863 **Fig. 1**

864 Regional geological map of the Ancestral Cascades arc, simplified from Schuster
865 (2005). The Ohanapecosh Formation is part of the Tertiary volcanoclastic formations.

866

867 **Fig. 2** Local geological map of the Ohanapecosh Formation in the Mt Rainier area;
868 simplified and slightly modified after Schuster (2005) and Fiske (1964). Logged
869 locations are white dots with letter. Thick black lines are boundaries between the
870 lithological associations of the Ohanapecosh Formation: Chinook Pass association
871 (A), White Pass association (B); Johnson Creek association (C). Dips are in the range
872 20–45° (Fiske et al., 1963). O.C. for Ohanapecosh campground.

873

874 **Fig. 3** Stratigraphy of the Chinook Pass association of the Ohanapecosh Formation at
875 Cayuse Pass (locality a in Figure 2) and Chinook Pass (localities b, c, d and e in
876 Figure 4). The proportions of clasts and matrix in representative samples of facies
877 were estimated in the field, and on polished rock slabs and thin sections in the
878 laboratory (Jutzeler, 2012). The log gives the mean clast diameter (i.e. most common
879 long-axis dimension of clasts) on the horizontal scale (in mm); some beds have
880 separate mean clast size for pumice clasts and fiamme (P) and dense clasts (D);
881 isolated clasts on right-hand side give outsized clast dimensions (i.e. maximum
882 dimension of the coarsest clast). Logs are in direct upward continuity from left to
883 right. Log locality (bold letter) refers to Figure 2; unit number (*italic type*), facies
884 number (**bold type**) and stratigraphic thickness (*plain type*) are given on the left-hand
885 side of logs; units (or group of units in thin facies) were separately numbered from
886 base to top of the logs. Pie diagrams give vol.% of different clast types from image
887 analysis (field and rock slabs): white for pumice clasts and fiamme, black for dense
888 clasts, gray for matrix (<2 mm), including crystal fragments. See electronic suppl. for
889 complete logs. For clarity, dykes and intrusions are not shown in the stratigraphic
890 logs. Dates are from U/Pb analyses on zircons by LA-ICP-MS; ages in brackets
891 suggest caution, as only one grain of zircon was used (see electronic suppl.).

892

893 **Fig. 4 a)** Simplified stratigraphic log of the Ohanapecosh Formation and Stevens
894 Ridge Member (Fifes Peak Formation) using sections at White Pass (1; localities l, m,
895 n and o in Figure 2), Ohanapecosh Campground (2; locality h in Figure 2) and
896 Backbone Ridge (3; localities i, j and k in Figure 2). Only dominant facies are
897 indicated; **b)** Inferred Ohanapecosh Fault; the fault repeats ~500 m of the White Pass
898 association (Ohanapecosh Formation) and the Stevens Ridge Member (Fifes Peak
899 Formation). The Stevens Ridge Member was dated at 25-27 Ma by Hammond (2011
900 unpubl. data). See electronic supplement for complete logs and U/Pb geochronology.

901

902 **Fig. 5** Facies 1 - Normally graded fiamme-dense clast breccia; **a)** Middle part of
903 facies 1 (unit 40) with porphyritic fiamme (black) and dense clasts (white and gray) in
904 a gray matrix; **b)** Basal facies 1 (unit 40, Cayuse Pass section) composed of dense
905 clasts, rare fiamme and feldspar crystal fragments (white) in a green matrix; **c)**
906 Typical stratigraphic log of facies 1 in unit 40, Cayuse Pass section. Dense clast (D),
907 fiamme (F), pumice clast (P), scoria (Sc), feldspar crystal (xl), cement (cem),
908 accretionary lapilli (al), mudstone (m); graphic log features and key as in Figure 3.

909

910 **Fig. 6** Facies 2 - Normally graded dense clast-fiamme breccia. **a)** Base of normally
911 graded dense clast-fiamme breccia (facies 2, unit 42, Cayuse Pass section) with sub-
912 rounded dark gray dense clasts in a gray matrix. This basal sub-facies is very similar
913 to the basal part of the normally graded fiamme-dense clast breccia (facies 1); **b)**
914 Stratigraphic log, unit 42, Cayuse Pass section. Graphic log features and key as in
915 Figures 3 and 5.

916

917 **Fig. 7** Facies 3 - Normally graded fiamme breccia. **a)** Base of unit 57 (Chinook Pass
918 section) in the Chinook Pass association. Abundant fiamme (pale green), minor dense
919 clasts (dark gray and black) in matrix; **b)** Stratigraphic log, unit 57, Chinook Pass
920 section. Graphic log features and key as in Figures 3 and 5.

921

922 **Fig. 8** Facies 4 - Reversely graded fiamme breccia. **a)** Unit 61 (Chinook Pass section)
923 overlying units 60a, 60b, 60c (reversely to normally graded pumice breccia, facies 8)
924 at Chinook Pass; top of unit 61 is not seen. Note the lateral continuity of the thin beds
925 and the knife sharp-contacts; **b)** Middle of unit 61 at Chinook Pass, with numerous
926 fiamme and pumice clasts (dark), rare dense clasts (white and pale gray) and feldspar
927 crystal fragments (white) in a pale matrix; **c)** Typical stratigraphic log of facies 4, unit
928 61, Chinook Pass section. Graphic log features and key as in Figures 3 and 5.

929

930 **Fig. 9** Facies 5 - Graded or massive volcanic breccia; **a)** Tube pumice clasts and dense
931 clasts in a fine (<0.2 mm) matrix (unit 5, White Pass section); **b)** Clast-supported
932 facies 5 at Indian Bar; pumice clasts and fiamme (dark), dense clasts and feldspar
933 crystals (white); **c)** Facies 5 at the base of the Ohanapecosh Formation (unit 5, White
934 Pass), dark fiamme, pumice clasts and dense clasts supported in a pale matrix; **d)**
935 Typical stratigraphic log of two beds of facies 5 in the White Pass section. Graphic
936 log features and key as in Figures 3 and 5.

937

938 **Fig. 10** Facies 6 - Massive volcanic breccia; **a)** Coarse volcanic breccia, White Pass
939 section (unit 62), composed of fine pumice clasts and fiamme (black) and dense
940 clasts, including a poorly vesicular basalt clast (bas); **b)** Typical stratigraphic log of
941 facies 6. Graphic log features and key as in Figures 3 and 5.

942

943 **Fig. 11** Facies 8 - Reversely to normally graded pumice breccia. **a)** Unit 60b, Chinook
944 Pass section. Note the reverse grading in pale gray pumice clasts in the lower unit, and
945 dark gray interbeds of mudstone; **b)** Reversely graded pumice clasts and mudstone
946 interbeds in facies 8 at Chinook Pass (unit 60); **c)** Sub-rounded pumice clasts (unit
947 60b); white zeolite cement fills interstices between pumice clasts; **d)** Two detailed
948 logs of laterally continuous units (60b and 60c) of facies 8 in the Chinook Pass
949 section. Log A is >80 m to the east of log B. The lines link the main parts of the two
950 sections that can be traced in the field. Graphic log features and key as in Figures 3
951 and 5.

952

953 **Fig. 12** Facies 9, Chinook Pass association (a, b) and White Pass association (c, d) -
954 Fine sandstone and mudstone. **a)** Succession of parallel-bedded facies 9 in lower
955 Cayuse Pass; **b)** Laminated facies 9 at Cougar Lake. Accretionary lapilli occur in
956 these beds. **c)** Beds of fine sandstone and mudstone (arrows, unit 78, White Pass)
957 interbedded with graded or massive volcanic breccia; **d)** Succession of very thin beds
958 and laminae of fine sandstone and mudstone (facies 9, unit D11 at Backbone Ridge);
959 fossil leaves were found in these beds. Key as in Figure 5.

960

961 **Fig. 13** Facies 11 - Basaltic scoria breccia. **a)** Thick, well bedded basaltic scoria
962 breccia (facies 11, lateral equivalent of bed 137) at White Pass. Note the upward arch
963 in the beds, interpreted to be primary dip. Cliff face (140-160°) is parallel to the
964 general bedding strike of the Ohanapecosh Formation. White circles for interpreted
965 impact sags, arrow for mafic sill. Inset gives a detailed view of an interpreted impact
966 sag; **b)** Unit 22 in the Ohanapecosh Campground section, with normally graded beds

967 of monomictic dark basaltic scoria clasts and pale-gray cement; **c)** Scanned slab of
968 facies 11 (unit 137 in the White Pass section), dark gray basaltic scoria clasts in pale
969 matrix and white zeolite cement; **d)** Stratigraphic log of unit 137, White Pass section.
970 Graphic log features and key as in Figures 3 and 5.

971

972 **Fig. 14** Inferred depositional processes in the Ohanapecosh Formation. **a)** Subaerial
973 magmatic gas-driven, pumice-forming explosive eruption (A) followed by collapse of
974 the eruption column and creation of magmatic gas-supported pyroclastic flow towards
975 water body (B). Coastal steam explosion (C) due to contact of hot pumice with water
976 (e.g. Cas and Wright, 1991; Freundt, 2003; Dufek et al., 2007). Accretionary lapilli
977 may form in subaerial eruption plumes. Dilute pyroclastic density current flows over
978 the water body (D). Pumice clasts from dilute pyroclastic density currents may stay
979 buoyant and create a pumice raft (E), to eventually generate saturation grading in
980 reversely to normally graded pumice breccia (facies 8). Dense part of the pyroclastic
981 flow enters water and transforms into a subaqueous volcanoclastic density current (F)
982 that deposits very thin to extremely thick, tabular beds (facies 1–5, 8, 9) on the basin
983 floor (G). Background sedimentation (H) produces fine grained thin beds (facies 9);
984 **b)** Mass-wasting processes (K) resediment unconsolidated aggregates, creating
985 subaqueous volcanoclastic density currents (L) that form tabular beds (facies 5–7, 9)
986 on the basin floor (M). Background sedimentation (H) produces interlayers of fine
987 grained thin beds (facies 9); **c)** Same resedimentation process (K) as in b, but in
988 shallower water, such as in the upper part of the White Pass association. Subaqueous
989 volcanoclastic density currents (N) generate tabular beds on the shallow basin floor
990 (O). Shallow intrusions of basalt (P; facies 12) and subaqueous to locally subaerial
991 eruptions (Q) build scoria cone of basaltic scoria breccia (R; facies 11) by subaerial

992 and water-settled fallout; thick proximal facies are affected by re sedimentation (S).
993 Scoria cone (R, facies 11) is discordant with general stratigraphy. Background
994 sedimentation and fallout from eruption column produces interlayers (T) of fine
995 grained thin beds (facies 9).

996

997 **Fig. 15**

998 Simplified stratigraphic logs of the Chinook Pass and White Pass associations
999 showing the contrasts between eruption-fed facies and re sedimented facies. See
1000 Figures 3 and 4 and electronic supplement for complete logs.

1001

1002 **Fig. 16**

1003 Reconstruction of the Ohanapecosh basin. Active subaerial andesitic volcanoes to the
1004 east supply most of the volcanoclastic facies preserved in the Ohanapecosh Formation.
1005 The depositional setting for most facies was subaqueous and below wave-base. Local
1006 intrabasinal scoria cones are present. The Chinook Pass association and White Pass
1007 association probably accumulated in two sub-basins, here separated by the thick gray
1008 dashed line. Flow-banded dacite at Cougar Lake not represented. Chinook Pass and
1009 Cayuse Pass, CP; Cougar Lake, CL; White Pass, WP; Backbone Ridge, BBR.

1010

1011 **TABLES**

1012 **Table 1** Textural characteristics of clasts in the Ohanapecosh Formation.

1013

1014 **Table 2** Lithofacies in the Ohanapecosh Formation.

1015

1016 **Table 3** Current type, origin and environment at source of main facies of the
1017 Ohanapecosh Formation.

1018

1019 **ELECTRONIC SUPPLEMENT**

1020

1021 **Additional field data**

1022 Chinook Pass and White Pass associations; GPS coordinates (WGS 84) of start,
1023 intermediary points and end of log section locations in the Ohanapecosh Formation.

1024

1025 **Fig. A** Complete stratigraphic log of Cayuse Pass section, Chinook Pass association;
1026 locality a in Figure 2. Logs are vertically continuous from left to right. Graphic log
1027 features and key as in Figures 3 and 5.

1028

1029 **Fig. B** Complete stratigraphic log of Chinook Pass section, Chinook Pass association;
1030 localities b, c and d in Figure 2. Logs are vertically continuous from left to right.
1031 Graphic log features and key as in Figures 3 and 5.

1032

1033 **Fig. C** Complete stratigraphic log of Cougar Lake section, Chinook Pass association;
1034 localities f and g in Figure 2. Graphic log features and key as in Figures 3 and 5.

1035

1036 **Fig. D** Complete stratigraphic log of White Pass section, White Pass association;
1037 localities l, m, n and o in Figure 2. Logs are vertically continuous from left to right.
1038 Graphic log features and key as in Figures 3 and 5.

1039

1040 **Fig. E** Complete stratigraphic log of Ohanapecosh campground section, White Pass
 1041 association; locality h in Figure 2. Logs are vertically continuous from left to right.
 1042 Graphic log features and key as in Figures 3 and 5.

1043

1044 **Fig. F** Complete stratigraphic log of Backbone Ridge section, White Pass association,
 1045 localities i, j and k in Figure 2. Logs are vertically continuous from left to right.
 1046 Graphic log features and key as in Figures 3 and 5.

1047

1048 **Fig. G** Typical stratigraphic log of the Johnson Creek association; locality p in Figure
 1049 2. Graphic log features and key as in Figures 3 and 5.

1050

1051 **REFERENCES**

- 1052 Allen, S. R., and Smith, I. E. M., 1994, Eruption styles and volcanic
 1053 hazard in the Auckland volcanic field, New Zealand:
 1054 Geoscience Reports of Shizuoka University = Shizuoka
 1055 Daigaku Chikyu Kagaku Kenkyu Hokoku, v. 20, p. 8-14.
- 1056 Allen, S. R., Simpson, C. J., McPhie, J., and Daly, S. J., 2003,
 1057 Stratigraphy, distribution and geochemistry of widespread
 1058 felsic volcanic units in the Mesoproterozoic Gawler Range
 1059 Volcanics, South Australia: Australian Journal of Earth
 1060 Sciences, v. 50, p. 97-112.
- 1061 Allen, S. R., 2004a, Complex spatter- and pumice-rich pyroclastic
 1062 deposits from an andesitic caldera-forming eruption: The Siwi
 1063 pyroclastic sequence, Tanna, Vanuatu: Bulletin of
 1064 Volcanology, v. 67, p. 27-41, doi: 10.1007/s00445-004-0358-
 1065 6.
- 1066 Allen, S. R., 2004b, The Parnell Grit beds revisited: Are they all the
 1067 products of sector collapse of western subaerial volcanoes of
 1068 the Northland Volcanic Arc?: New Zealand Journal of Geology
 1069 and Geophysics, v. 47, p. 509-524.
- 1070 Allen, S. R., and Freundt, A., 2006, Resedimentation of cold
 1071 pumiceous ignimbrite into water: Facies transformations
 1072 simulated in flume experiments: Sedimentology, v. 53, p.
 1073 717-734, doi: 10.1111/j.1365-3091.2006.00790.x.
- 1074 Allen, S. R., Hayward, B. W., and Mathews, E., 2007, A facies model
 1075 for a submarine volcanoclastic apron: The Miocene Manukau

- 1076 Subgroup, New Zealand: Geological Society of America
1077 Bulletin, v. 119, p. 725-742, doi: 10.1111/j.1365-
1078 3091.2006.00790.x.
- 1079 Allen, S. R., Fiske, R. S., and Cashman, K. V., 2008, Quenching of
1080 steam-charged pumice; implications for submarine pyroclastic
1081 volcanism: Earth and Planetary Science Letters, v. 274, p. 40-
1082 49, doi: 10.1016/j.epsl.2008.06.050.
- 1083 Allen, S. R., and McPhie, J., 2009, Products of neptunian eruptions:
1084 Geology, v. 37, p. 639-642, doi: 10.1130/G30007A.1.
- 1085 Allen, S. R., Freundt, A., and Kurokawa, K., 2012, Characteristics of
1086 submarine pumice-rich density current deposits sourced from
1087 turbulent mixing of subaerial pyroclastic flows at the
1088 shoreline: field and experimental assessment: Bulletin of
1089 Volcanology, v. 74, p. 657-675, doi: 10.1007/s00445-011-
1090 0553-1.
- 1091 Armstrong, R. L., and Ward, P., 1991, Evolving geographic patterns
1092 of Cenozoic magmatism in the North American Cordillera: the
1093 temporal and spatial association of magmatism and
1094 metamorphic core complexes: Journal of Geophysical
1095 Research, v. 96, p. 13201-13224, doi: 10.1029/91JB00412.
- 1096 Bacon, C. R., 1983, Eruptive history of Mount Mazama and Crater
1097 Lake caldera, Cascade Range, USA: Journal of Volcanology
1098 and Geothermal Research, v. 18, p. 57-115.
- 1099 Bailey, R. A., Dalrymple, G. B., and Lanphere, M. A., 1976,
1100 Volcanism, structure, and geochronology of Long Valley
1101 caldera, Mono County, California: Journal of Geophysical
1102 Research, v. 81, p. 725-744, doi: 10.1029/JB081i005p00725.
- 1103 Baltzer, F., 1991, Late Pleistocene and Recent detrital
1104 sedimentation in the deep parts of northern Lake Tanganyika
1105 (East African Rift), *in* Anadon, P., Cabrera, L., and Kelts, K.,
1106 eds., Lacustrine facies analysis: Oxford, England, Blackwell, p.
1107 147-173.
- 1108 Blakely, R. J., Wells, R. E., Weaver, C. S., and Johnson, S. Y., 2002,
1109 Location, structure, and seismicity of the Seattle fault zone,
1110 Washington: Evidence from aeromagnetic anomalies, geologic
1111 mapping, and seismic-reflection data: Geological Society of
1112 America Bulletin, v. 114, p. 169-177.
- 1113 Bonini, W. E., Hughes, D. W., and Danes, Z. F., 1974, Complete
1114 bouguer gravity anomaly map of Washington: Washington
1115 Department of Natural Resources Division of Geology and
1116 Earth Resources scale 1:500,000.
- 1117 Boulter, C. A., 1987, Subaqueous deposition of accretionary lapilli:
1118 significance for palaeoenvironmental interpretations in
1119 Archaean greenstone belts: Precambrian Research, v. 34, p.
1120 231-246.

- 1121 Bouma, A. H., 1962, Sedimentology of some flysch deposits; a
1122 graphic approach to facies interpretation: Amsterdam,
1123 Elsevier, 168 p.
- 1124 Bryan, S. E., Cook, A., Evans, J. P., Colls, P. W., Wells, M. G.,
1125 Lawrence, M. G., Jell, J. S., Greig, A., and Leslie, R., 2004,
1126 Pumice rafting and faunal dispersion during 2001-2002 in the
1127 Southwest Pacific: Record of a dacitic submarine explosive
1128 eruption from Tonga: *Earth and Planetary Science Letters*, v.
1129 227, p. 135-154, doi: 10.1016/j.epsl.2004.08.009.
- 1130 Bull, K. F., and McPhie, J., 2007, Fiamme textures in volcanic
1131 successions: Flaming issues of definition and interpretation:
1132 *Journal of Volcanology and Geothermal Research*, v. 164, p.
1133 205-216, doi: 10.1016/j.jvolgeores.2007.05.005.
- 1134 Burgisser, A., and Gardner, J. E., 2006, Using hydraulic
1135 equivalences to discriminate transport processes of volcanic
1136 flows: *Geology*, v. 34, p. 157-160, doi: 10.1130/G21942.1.
- 1137 Busby-Spera, C., 1985, A sand-rich submarine fan in the lower
1138 Mesozoic Mineral King Caldera Complex, Sierra Nevada,
1139 California: *Journal of Sedimentary Petrology*, v. 55, p. 376-
1140 391.
- 1141 Busby-Spera, C. J., 1986, Depositional features of rhyolitic and
1142 andesitic volcanoclastic rocks of the Mineral King submarine
1143 caldera complex, Sierra Nevada, California: *Journal of*
1144 *Volcanology and Geothermal Research*, v. 27, p. 43-76.
- 1145 Busby-Spera, C. J., 1988, Evolution of a Middle Jurassic back-arc
1146 basin, Cedros Island, Baja California; evidence from a marine
1147 volcanoclastic apron: *Geological Society of America Bulletin*, v.
1148 100, p. 218-233.
- 1149 Busby, C., Fackler Adams, B., Mattinson, J., and Deoreo, S., 2006,
1150 View of an intact oceanic arc, from surficial to mesozonal
1151 levels: Cretaceous Alisitos arc, Baja California: *Journal of*
1152 *Volcanology and Geothermal Research*, v. 149, p. 1-46.
- 1153 Busby, C. J., Bassett, K. N., Steiner, M. B., and Riggs, N. R., 2005,
1154 Climatic and tectonic controls on Jurassic intra-arc basins
1155 related to northward drift of North America, p. 359-376.
- 1156 Busby, C. J., and Bassett, K. N., 2007, Volcanic facies architecture
1157 of an intra-arc strike-slip basin, Santa Rita Mountains,
1158 Southern Arizona: *Bulletin of Volcanology*, v. 70, p. 85-103.
- 1159 Busby, C. J., 2012, Extensional and transtensional continental arc
1160 basins: case studies from the southwestern United States, *in*
1161 Busby, C. J., and Azor, A., eds., *Tectonics of Sedimentary*
1162 *Basins: Recent Advances*, Blackwell Publishing Ltd., p. 382-
1163 404.
- 1164 Carey, S., Sigurdsson, H., Mandeville, C., and Bronto, S., 1996,
1165 Pyroclastic flows and surges over water: An example from the
1166 1883 Krakatau eruption: *Bulletin of Volcanology*, v. 57, p.
1167 493-511.

- 1168 Cas, R. A. F., and Wright, J. V., 1991, Subaqueous pyroclastic flows
1169 and ignimbrites: an assessment: *Bulletin of Volcanology*, v.
1170 53, p. 357-380, doi: 10.1007/BF00280227.
- 1171 Cashman, K. V., and Fiske, R. S., 1991, Fallout of pyroclastic debris
1172 from submarine volcanic eruptions: *Science*, v. 253, p. 275-
1173 280, doi: 10.1126/science.253.5017.275.
- 1174 Cheney, E. S., and Hayman, N. W., 2009, The Chiwaukum
1175 Structural Low; Cenozoic shortening of the central Cascade
1176 Range, Washington State, USA: *Geological Society of America
1177 Bulletin*, v. 121, p. 1135-1153, doi: 10.1130/B26446.1.
- 1178 Colgan, J. P., Egger, A. E., John, D. A., Cousens, B., Fleck, R. J.,
1179 and Henry, C. D., 2011, Oligocene and Miocene arc volcanism
1180 in northeastern California: Evidence for post-Eocene
1181 segmentation of the subducting Farallon plate: *Geosphere*, v.
1182 7, p. 733-755, doi: 10.1130/GES00650.1.
- 1183 Crandell, D. R., 1976, *The geologic story of Mount Rainier*: U.S.
1184 Geological Survey, B 1292.
- 1185 Dickinson, W. R., 2009, Anatomy and global context of the North
1186 American Cordillera, *in* Kay, S. M., Ramos, Victor A.,
1187 Dickinson, William R., ed., *Memoirs of the Geological Society
1188 of America*: Boulder, Colorado, Geological Society of America
1189 (GSA), p. 1-29.
- 1190 du Bray, E. A., John, D. A., Sherrod, D. R., Evarts, R. C., Conrey, R.
1191 M., and Lexa, J., 2006, *Geochemical database for volcanic
1192 rocks of the western Cascades, Washington, Oregon, and
1193 California*: U. S. Geological Survey Data Series, p. 49-49.
- 1194 du Bray, E. A., and John, D. A., 2011, Petrologic, tectonic, and
1195 metallogenic evolution of the Ancestral Cascades magmatic
1196 arc, Washington, Oregon, and northern California: *Geosphere*,
1197 v. 7, p. 1102-1133, doi: 10.1130/GES00669.1.
- 1198 Dufek, J., Manga, M., and Staedter, M., 2007, Littoral blasts:
1199 Pumice-water heat transfer and the conditions for steam
1200 explosions when pyroclastic flows enter the ocean: *Journal of
1201 Geophysical Research, [Solid Earth and Planets]*, v. 112, p.
1202 B11201, doi: 10.1029/2006JB004910.
- 1203 Dufek, J., and Manga, M., 2008, In situ production of ash in
1204 pyroclastic flows: *Journal of Geophysical Research, [Solid
1205 Earth and Planets]*, v. 113, p. B09207, doi:
1206 10.1029/2007JB005555.
- 1207 Edmonds, M., and Herd, R. A., 2005, Inland-directed base surge
1208 generated by the explosive interaction of pyroclastic flows and
1209 seawater at Soufrière Hills volcano, Montserrat: *Geology*, v.
1210 33, p. 245-248, doi: 10.1130/G21166.1.
- 1211 Ellingson, J. A., 1972, *The rocks and structure of the White Pass
1212 area, Washington*: Northwest Science, v. 46, p. 9-24.
- 1213 Evans, J. E., 2010, *The Chiwaukum Structural Low: Cenozoic
1214 shortening of the central Cascade Range, Washington State,*

- 1215 USA: Comment: Geological Society of America Bulletin, v.
1216 122, p. 2097-2102, doi: 10.1130/B30152.1.
- 1217 Evarts, R. C., Ashley, R. P., and Smith, J. G., 1987, Geology of the
1218 Mount St. Helens area: record of discontinuous volcanic and
1219 plutonic activity in the Cascade arc of southern Washington
1220 (USA): Journal of Geophysical Research, v. 92, p. 10155-
1221 10169, doi: 10.1029/JB092iB10p10155.
- 1222 Expedition 340 Scientists, 2012, Lesser Antilles volcanism and
1223 landslides: implications for hazard assessment and long-term
1224 magmatic evolution of the arc: IODP Preliminary Report, v.
1225 340, doi: 10.2204/iodp.pr.340.2012.
- 1226 Fisher, R. V., 1961a, Stratigraphy of the Ashford area, southern
1227 Cascades, Washington: Geological Society of America Bulletin,
1228 v. 72, p. 1395-1407, doi: 10.1130/0016-
1229 7606(1961)72[1395:SOTAAS]2.0.CO; 2
- 1230 Fisher, R. V., 1961b, Proposed classification of volcanoclastic
1231 sediments and rocks: Geological Society of America Bulletin,
1232 v. 72, p. 1409-1414, doi: 10.1130/0016-7606(1961)
1233 72[1409:PCOVSA]2.0.CO; 2
- 1234 Fisher, R. V., and Schmincke, H.-U., 1984, Pyroclastic rocks: Berlin,
1235 Federal Republic of Germany (DEU), Springer-Verlag, 472 p.
- 1236 Fiske, R. S., 1963, Subaqueous pyroclastic flows in the
1237 Ohanapecoh Formation, Washington: Geological Society of
1238 America Bulletin, v. 74, p. 391-406, doi: 10.1130/0016-
1239 7606(1963)74[391:SPFITO]2.0.CO; 2
- 1240 Fiske, R. S., Hopson, C. A., and Waters, A. C., 1963, Geology of
1241 Mount Rainier National Park, Washington: U.S. Geological
1242 Survey Professional Paper, v. 444, p. 93.
- 1243 Fiske, R. S., Hopson, C. A., and Waters, A. C., 1964, Geologic map
1244 and section of Mount Rainier National Park, Washington, scale
1245 1:62,500.
- 1246 Freundt, A., 2003, Entrance of hot pyroclastic flows into the sea:
1247 Experimental observations: Bulletin of Volcanology, v. 65, p.
1248 144-164.
- 1249 Frizzell, V. A., Jr., Tabor, R. W., Booth, D. B., Ort, K. M., and Waitt,
1250 R. B., Jr., 1984, Preliminary geologic map of the Snoqualmie
1251 Pass 1:100,000 Quadrangle, Washington: U. S. Geological
1252 Survey, OF 84-0693.
- 1253 Gard, L. M., Jr., 1968, Bedrock geology of the Lake Tapps
1254 Quadrangle, Pierce County, Washington: U. S. Geological
1255 Survey, P 0388-B.
- 1256 Gaylord, D. R., Price, S. M., and Suydam, J. D., 2001, Volcanic and
1257 hydrothermal influences on middle Eocene lacustrine
1258 sedimentary deposits, Republic Basin, northern Washington,
1259 USA, *in* White, J. D. L., and Riggs, N. R., eds., Volcanoclastic
1260 Sedimentation in Lacustrine Settings: Oxford, England,
1261 Blackwell Science, p. 199-222.

- 1262 Hammond, P. E., 1979, A tectonic model for evolution of the
1263 Cascade Range, *in* Armentrout, J. M., Cole, M. R., and
1264 TerBest, H., Jr., eds., Pacific Coast Paleogeography
1265 Symposium, no.3: Society of Economic Paleontologists and
1266 Mineralogists, Pacific Section, p. 219-237.
- 1267 Hammond, P. E., 2005, Geologic map of the Timberwolf Mountain
1268 7.5 minute Quadrangle, Yakima County, Washington:
1269 Washington State Department of Natural Resources, division
1270 of Geology and Earth Resources, scale 1:24,000.
- 1271 Hammond, P. E., 2011 unpubl. data.
- 1272 Head, J. W., and Wilson, L., 2003, Deep submarine pyroclastic
1273 eruptions: Theory and predicted landforms and deposits:
1274 Journal of Volcanology and Geothermal Research, v. 121, p.
1275 155-193.
- 1276 Hildreth, W., 2007, Quaternary magmatism in the Cascades;
1277 geologic perspectives: U.S. Geological Survey Professional
1278 Paper, v. P 1744, p. 125.
- 1279 Ingram, R. L., 1954, Terminology for the thickness of stratification
1280 and parting units in sedimentary rocks: Geological Society of
1281 America Bulletin, v. 65, p. 937-938, doi: 10.1130/0016-
1282 7606(1954)65[937:TFTTOS]2.0.CO;2
- 1283 Johnson, H. D., and Baldwin, C. T., 1996, Shallow clastic seas, *in*
1284 Reading, H. G., and Johnson, H. D., eds., Sedimentary
1285 environments; processes, facies and stratigraphy: United
1286 Kingdom (GBR), Blackwell Science, Oxford, p. 232-280.
- 1287 Johnson, S. Y., 1985, Eocene strike-slip faulting and non-marine
1288 basin formation in Washington, *in* Biddle, K. T., and Christie-
1289 Blick, N., eds., Strike-slip deformation, basin formation, and
1290 sedimentation: Tulsa; OK, SEPM (Society for Sedimentary
1291 Geology), p. 283-302.
- 1292 Johnson, T. C., 1984, Sedimentation in large lakes (chemical
1293 processes): Annual Review of Earth and Planetary Sciences, v.
1294 12, p. 179-204.
- 1295 Jutzeler, M., 2012, Characteristics and origin of subaqueous
1296 pumice-rich pyroclastic facies: Ohanapecosh Formation (USA)
1297 and Dogashima Formation (Japan). [Ph.D. thesis]: University
1298 of Tasmania, 205 p.
- 1299 Jutzeler, M., Proussevitch, A. A., and Allen, S. R., 2012, Grain-size
1300 distribution of volcanoclastic rocks 1: A new technique based
1301 on functional stereology: Journal of Volcanology and
1302 Geothermal Research, v. 239-240, p. 1-11, doi:
1303 10.1016/j.jvolgeores.2012.05.013.
- 1304 Kano, K., 2003, Subaqueous pumice eruptions and their products; a
1305 review, *in* White, J. D. L., Smellie, J. L., and Clague, D. A.,
1306 eds., Explosive Subaqueous Volcanism: Washington, D.C.,
1307 AGU, p. 213-230.

- 1308 Kokelaar, B. P., 1983, The mechanism of Surtseyan volcanism:
1309 Journal of the Geological Society [London], v. 140, p. 939-
1310 944.
- 1311 Kokelaar, P., 1986, Magma-water interactions in subaqueous and
1312 emergent basaltic: Bulletin of Volcanology, v. 48, p. 275-289.
- 1313 Kokelaar, P., Raine, P., and Branney, M. J., 2007, Incursion of a
1314 large-volume, spatter-bearing pyroclastic density current into
1315 a caldera lake: Pavey Ark ignimbrite, Scafell caldera, England:
1316 Bulletin of Volcanology, v. 70, p. 23-54, doi: 10.1007/s00445-
1317 007-0118-5.
- 1318 Kurokawa, K., and Tomita, Y., 1998, The Znp-Ohta ash; an early
1319 Pliocene widespread subaqueous tephra deposit in central
1320 Japan: Chishitsugaku Zasshi = Journal of the Geological
1321 Society of Japan, v. 104, p. 558-561.
- 1322 Legros, F., and Druitt, T. H., 2000, On the emplacement of
1323 ignimbrite in shallow-marine environments: Journal of
1324 Volcanology and Geothermal Research, v. 95, p. 9-22.
- 1325 Lowe, D. R., 1982, Sediment gravity flows: II. Depositional models
1326 with special reference to the deposits of high-density turbidity
1327 currents: Journal of Sedimentary Petrology, v. 52, p. 279-
1328 297.
- 1329 Mandeville, C. W., Carey, S., and Sigurdsson, H., 1996,
1330 Sedimentology of the Krakatau 1883 submarine pyroclastic
1331 deposits: Bulletin of Volcanology, v. 57, p. 512-529.
- 1332 Manga, M., Patel, A., and Dufek, J., 2011, Rounding of pumice
1333 clasts during transport: Field measurements and laboratory
1334 studies: Bulletin of Volcanology, v. 73, p. 321-333, doi:
1335 10.1007/s00445-010-0411-6.
- 1336 Manville, V., White, J. D. L., Houghton, B. F., and Wilson, C. J. N.,
1337 1998, The saturation behaviour of pumice and some
1338 sedimentological implications: Sedimentary Geology, v. 119,
1339 p. 5-16, doi: 10.1016/S0037-0738(98)00057-8.
- 1340 Manville, V., 2001, Sedimentology and history of Lake Reporoa; an
1341 ephemeral supra-ignimbrite lake, Taupo volcanic zone, New
1342 Zealand, *in* White, J. D. L., and Riggs, N. R., eds.,
1343 Volcaniclastic Sedimentation in Lacustrine Settings: Oxford,
1344 England, Blackwell Science, p. 109-140.
- 1345 Manville, V., Segschneider, B., and White, J. D. L., 2002,
1346 Hydrodynamic behaviour of Taupo 1800a pumice:
1347 Implications for the sedimentology of remobilized pyroclasts:
1348 Sedimentology, v. 49, p. 955-976.
- 1349 McBirney, A. R., 1978, Volcanic evolution of the Cascade Range:
1350 Annual Review of Earth and Planetary Sciences, v. 6, p. 437-
1351 456.
- 1352 McPhie, J., Doyle, M., and Allen, R., 1993, Volcanic Textures:
1353 Hobart, Australia, ARC- Centre of Excellence in Ore Deposits
1354 University of Tasmania, 198 p.

- 1355 Mulder, T., and Alexander, J., 2001, The physical character of
1356 subaqueous sedimentary density flow and their deposits:
1357 *Sedimentology*, v. 48, p. 269-299, doi: 10.1046/j.1365-
1358 3091.2001.00360.x.
- 1359 Piper, D. J. W., and Normark, W. R., 2009, Processes that initiate
1360 turbidity currents and their influence on turbidites; a marine
1361 geology perspective: *Journal of Sedimentary Research*, v. 79,
1362 p. 347-362, doi: 10.2110/isr.2009.046.
- 1363 Platt, N. H., and Wright, V. P., 1991, Lacustrine carbonates: facies
1364 models, facies distributions and hydrocarbon aspects, *in*
1365 Anadon, P., Cabrera, L., and Kelts, K., eds., *Lacustrine facies*
1366 *analysis*: Oxford, England, Blackwell Scientific, p. 57-74.
- 1367 Reiners, P. W., Ehlers, T. A., Garver, J. I., Mitchell, S. G.,
1368 Montgomery, D. R., Vance, J. A., and Nicolescu, S., 2002,
1369 Late Miocene exhumation and uplift of the Washington
1370 Cascade Range: *Geology*, v. 30, p. 767-770, doi:
1371 10.1130/0091-7613(2002)030<0767:LMEAUO>2.0.CO;2.
- 1372 Rubey, W. W., 1933, The size distribution of heavy minerals within
1373 a water-laid sandstone: *Journal of Sedimentary Petrology*, v.
1374 3, p. 3-29.
- 1375 Sadler, P. M., 1981, Sediment accumulation rates and the
1376 completeness of stratigraphic sections: *Journal of Geology*, v.
1377 89, p. 569-584.
- 1378 Schasse, H. W., 1987, Geologic map of the Mount Rainier
1379 quadrangle, Washington: Division of Geology and Earth
1380 Resources, 87-16.
- 1381 Schumacher, R., and Schmincke, H. U., 1991, Internal structure
1382 and occurrence of accretionary lapilli - a case study at Laacher
1383 See Volcano: *Bulletin of Volcanology*, v. 53, p. 612-634, doi:
1384 10.1007/BF00493689.
- 1385 Schuster, J. E., 2005, Geologic map of Washington state, GM-53:
1386 Washington State Department of Natural Resources Division
1387 of Geology and Earth Resources, scale 1:500,000.
- 1388 Shanmugam, G., 2002, Ten turbidite myths: *Earth-Science*
1389 *Reviews*, v. 58, p. 311-341, doi: 10.1016/S0012-
1390 8252(02)00065-X.
- 1391 Sherrod, D. R., and Smith, J. G., 2000, Geologic map of upper
1392 Eocene to Holocene volcanic and related rocks of the Cascade
1393 Range, Oregon: U. S. Geological Survey, Reston, VA.
- 1394 Simmons, G. C., Van Noy, R. M., and Zilka, N. T., 1983, Mineral
1395 resources of the Cougar Lakes-Mount Aix study area, Yakima
1396 and Lewis counties, Washington: U.S. Geological Survey
1397 *Bulletin*, v. 1504.
- 1398 Smith, G. A., 1991, Facies sequences and geometries in continental
1399 volcanoclastic sediments: Special Publication - Society of
1400 Economic Paleontologists and Mineralogists, v. 45, p. 109-
1401 121.

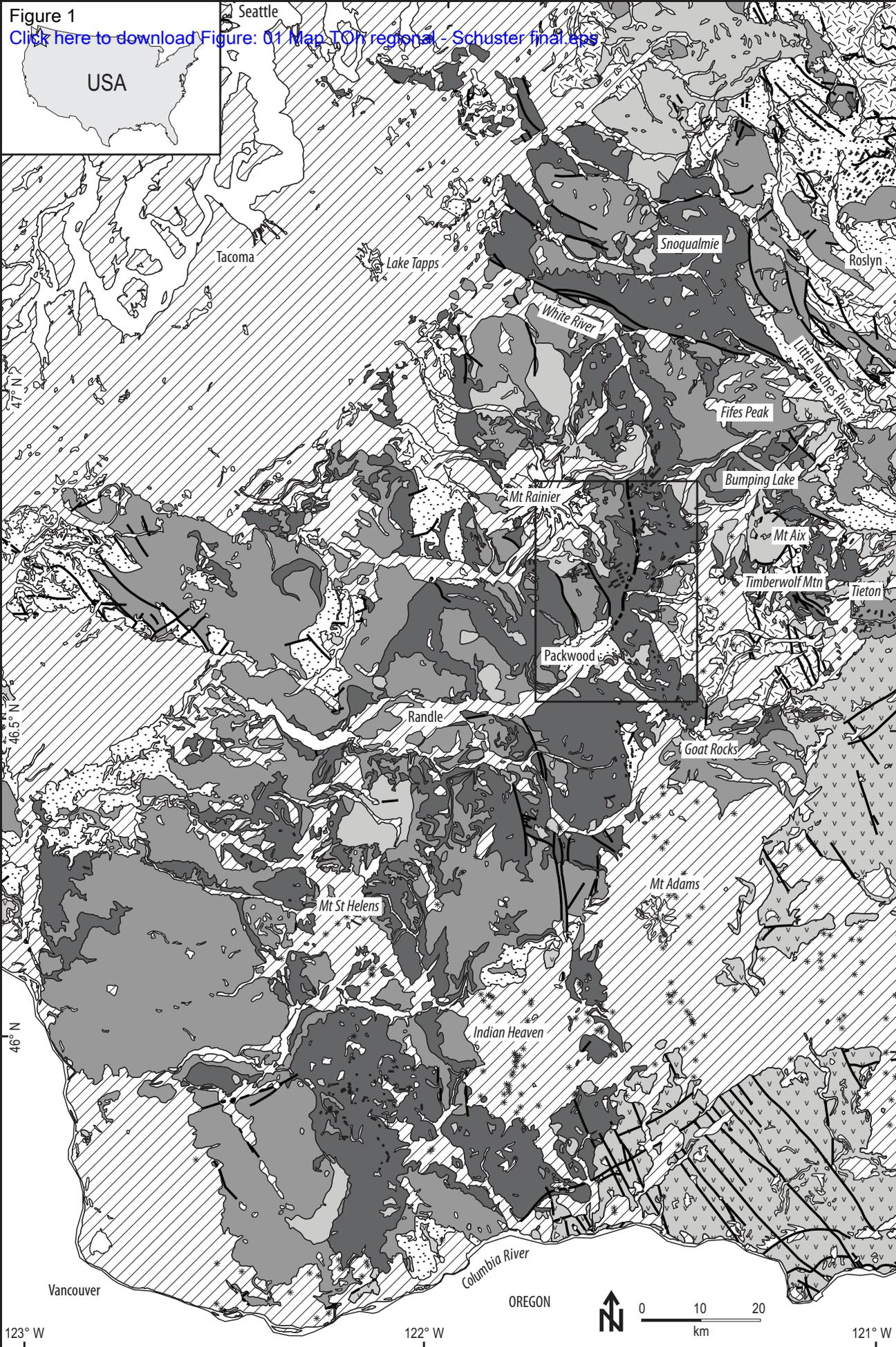
- 1402 Smith, J. G., 1989, Geologic map of upper Eocene to Holocene
1403 volcanic and related rocks in the Cascade Range, Washington:
1404 U. S. Geological Survey, Open-File Report 89-0311.
- 1405 Sohn, Y. K., Park, K. H., and Yoon, S. H., 2008, Primary versus
1406 secondary and subaerial versus submarine hydrovolcanic
1407 deposits in the subsurface of Jeju Island, Korea:
1408 *Sedimentology*, v. 55, p. 899-924.
- 1409 Sparks, R. S. J., Sigurdsson, H., and Carey, S. N., 1980, The
1410 entrance of pyroclastic flows into the sea; I, Oceanographic
1411 and geologic evidence from Dominica, Lesser Antilles;
1412 Explosive volcanism in island arcs: *Journal of Volcanology and*
1413 *Geothermal Research*, v. 7, p. 87-96.
- 1414 Stine, C. M., 1987, Stratigraphy of the Ohanapecosh formation
1415 North of Hamilton Buttes, Southcentral Washington [M.Sc.
1416 thesis]: Portland State University, 83 p.
- 1417 Stow, D. A. V., Reading, H. G., and Collinson, J. D., 1996, Deep
1418 seas, *in* Reading, H. G., ed., *Sedimentary environments;*
1419 *processes, facies and stratigraphy*: Oxford, Blackwell Science,
1420 p. 395-453.
- 1421 Sumner, E. J., Talling, P. J., and Amy, L. A., 2009, Deposits of flows
1422 transitional between turbidity current and debris flow:
1423 *Geology*, v. 37, p. 991-994, doi: 10.1130/G30059A.1.
- 1424 Swanson, D. A., 1965, The middle and late Cenozoic volcanic rock
1425 of the Tieton River area, south-central Washington [Ph.D.
1426 thesis]: Johns Hopkins University, 333 p.
- 1427 Swanson, D. A., 1966, Tieton volcano, a Miocene eruptive center in
1428 the Southern Cascade Mountains, Washington: *Geological*
1429 *Society of America Bulletin*, v. 77, p. 1293-1314, doi:
1430 10.1130/0016-7606(1966)77[1293:TVAMEC]2.0.CO;2.
- 1431 Swanson, D. A., 1978, Geologic map of the Tieton River area,
1432 Yakima County, South-central Washington: U. S. Geological
1433 Survey, MF- 968.
- 1434 Swanson, D. A., 1996, Geologic map of the Packwood Lake
1435 Quadrangle, southern Cascade Range, Washington: U. S.
1436 Geological Survey, OF 96-0704.
- 1437 Swanson, D. A., Moore, R. B., and Banks, N. G., 1997, Geologic
1438 map of the Packwood Quadrangle, southern Cascade Range,
1439 Washington: U. S. Geological Survey, OF 97-0157.
- 1440 Tabor, R. W., Frizzell, V. A., Jr., Vance, J. A., and Naeser, C. W.,
1441 1984, Ages and stratigraphy of lower and middle Tertiary
1442 sedimentary and volcanic rocks of the central Cascades,
1443 Washington; application to the tectonic history of the Straight
1444 Creek Fault: *Geological Society of America Bulletin*, v. 95, p.
1445 26-44, doi: 10.1130/0016-
1446 7606(1984)95<26:AASOLA>2.0.CO;2

- 1447 Tabor, R. W., Frizzell, V. A., Jr., Booth, D. B., and Waitt, R. B.,
1448 2000, Geologic map of the Snoqualmie Pass 30x60 minute
1449 quadrangle, Washington: U. S. Geological Survey, I-2538.
- 1450 Talling, P. J., Masson, D. G., Sumner, E. J., and Malgesini, G., 2012,
1451 Subaqueous sediment density flows: Depositional processes
1452 and deposit types: *Sedimentology*, v. 59, p. 1937-2003.
- 1453 Trofimovs, J., Amy, L., Boudon, G., Deplus, C., Doyle, E., Fournier,
1454 N., Hart, M. B., Komorowski, J. C., Le Friant, A., Lock, E. J.,
1455 Pudsey, C., Ryan, G., Sparks, R. S. J., and Talling, P. J.,
1456 2006, Submarine pyroclastic deposits formed at the Soufrière
1457 Hills volcano, Montserrat (1995-2003): What happens when
1458 pyroclastic flows enter the ocean?: *Geology*, v. 34, p. 549-
1459 552, doi: 10.1130/G22424.1.
- 1460 Vance, J. A., Clayton, G. A., Mattinson, J. M., and Naeser, C. W.,
1461 1987, Early and middle Cenozoic stratigraphy of the Mount
1462 Rainier-Tieton River area, southern Washington Cascades:
1463 Bulletin - Washington, Division of Geology and Earth
1464 Resources, v. 77, p. 269-290.
- 1465 Warren, W. C., 1941, Relation of the Yakima basalt to the Keechelus
1466 andesitic series [Washington]: *Journal of Geology*, v. 49, p.
1467 795-814.
- 1468 White, J. D. L., and Busby-Spera, C. J., 1987, Deep marine arc
1469 apron deposits and syndepositional magmatism in the Alisitos
1470 Group at Punta Cono, Baja California, Mexico: *Sedimentology*,
1471 v. 34, p. 911-927.
- 1472 White, J. D. L., 2000, Subaqueous eruption-fed density currents and
1473 their deposits: *Precambrian Research*, v. 101, p. 87-109, doi:
1474 10.1016/S0301-9268(99)00096-0.
- 1475 White, J. D. L., 2001, Eruption and reshaping of Pahvant Butte
1476 Volcano in Pleistocene Lake Bonneville, *in* White, J. D. L., and
1477 Riggs, N. R., eds., *Volcaniclastic Sedimentation in Lacustrine
1478 Settings*: Oxford, England, Blackwell Science, p. 61-80.
- 1479 White, J. D. L., Manville, V., Wilson, C. J. N., Houghton, B. F., Riggs,
1480 N. R., and Ort, M., 2001, Settling and deposition of AD 181
1481 Taupo pumice in lacustrine and associated environments, *in*
1482 White, J. D. L., and Riggs, N. R., eds., *Volcaniclastic
1483 Sedimentation in Lacustrine Settings*: Oxford, England,
1484 Blackwell Science, p. 141-150.
- 1485 White, J. D. L., Smellie, J. L., and Clague, D. A., 2003, Introduction:
1486 A deductive outline and topical overview of subaqueous
1487 explosive volcanism, *in* White, J. D. L., Smellie, J. L., and
1488 Clague, D. A., eds., *Explosive Subaqueous Volcanism*:
1489 Washington, D.C., AGU, p. 1-23.
- 1490 Whitham, A. G., and Sparks, R. S. J., 1986, Pumice: *Bulletin of
1491 Volcanology*, v. 48, p. 209-223, doi: 10.1007/BF01087675.
- 1492 Whitham, A. G., 1989, The behaviour of subaerially produced
1493 pyroclastic flows in a subaqueous environment: Evidence from

- 1494 the Roseau eruption, Dominica, West Indies: *Marine Geology*,
1495 v. 86, p. 27-40.
- 1496 Wiesner, M. G., Yubo, W., and Lianfu, Z., 1995, Fallout of volcanic
1497 ash to the deep South China Sea induced by the 1991
1498 eruption of Mount Pinatubo (Philippines): *Geology*, v. 23, p.
1499 885-888.
- 1500 Winters, W. J., 1984, Stratigraphy and sedimentology of Paleogene
1501 arkosic and volcanoclastic strata, Johnson Creek-Chambers
1502 Creek area, southern Cascade Range, Washington [M.Sc.
1503 thesis]: Portland State University, 160 p.
- 1504 Wise, W. S., 1970, Cenozoic volcanism in the Cascade Mountains of
1505 southern Washington: Washington (State) Department of
1506 Natural Resources Division of Geology and Earth Resources,
1507 0096-6045.
- 1508 Yamada, E., 1984, Subaqueous pyroclastic flows: their development
1509 and their deposits, *in* Kokelaar, B. P., and Howells, M. F.,
1510 eds., *Marginal basin geology*, Blackwell Scientific, p. 29-35.
1511
1512

Figure 1

[Click here to download Figure: 01 Map TOH regional - Schuster final.tps](#)



- | | | | |
|-----------------------------|---|-----------------------------|--|
| Water and ice | Tertiary intrusion | Tertiary non-volcanic units | Fault |
| Quaternary | Tertiary volcanic units | Mesozoic and Pre-Cambrian | Ohanapetosh Fault (inferred; this study) |
| Columbia River Basalt Group | Tertiary volcaniclastic units, including the Ohanapetosh Fm | Quaternary vent | |

Figure 2
[Click here to download Figure_02 Map TOh study eps](#)

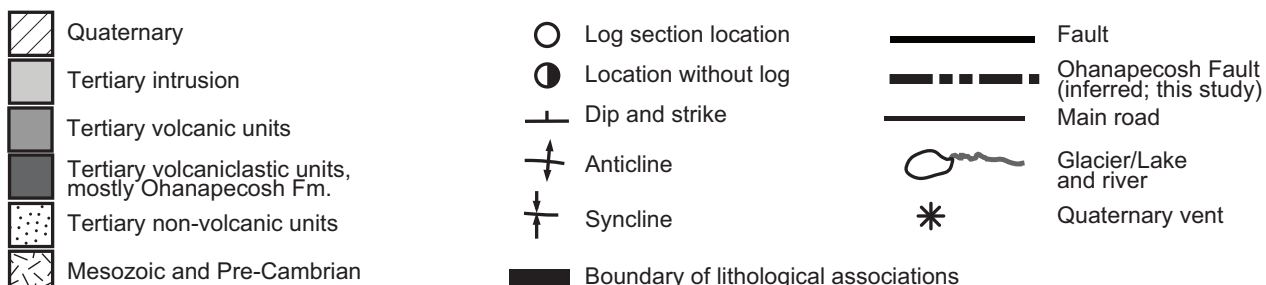
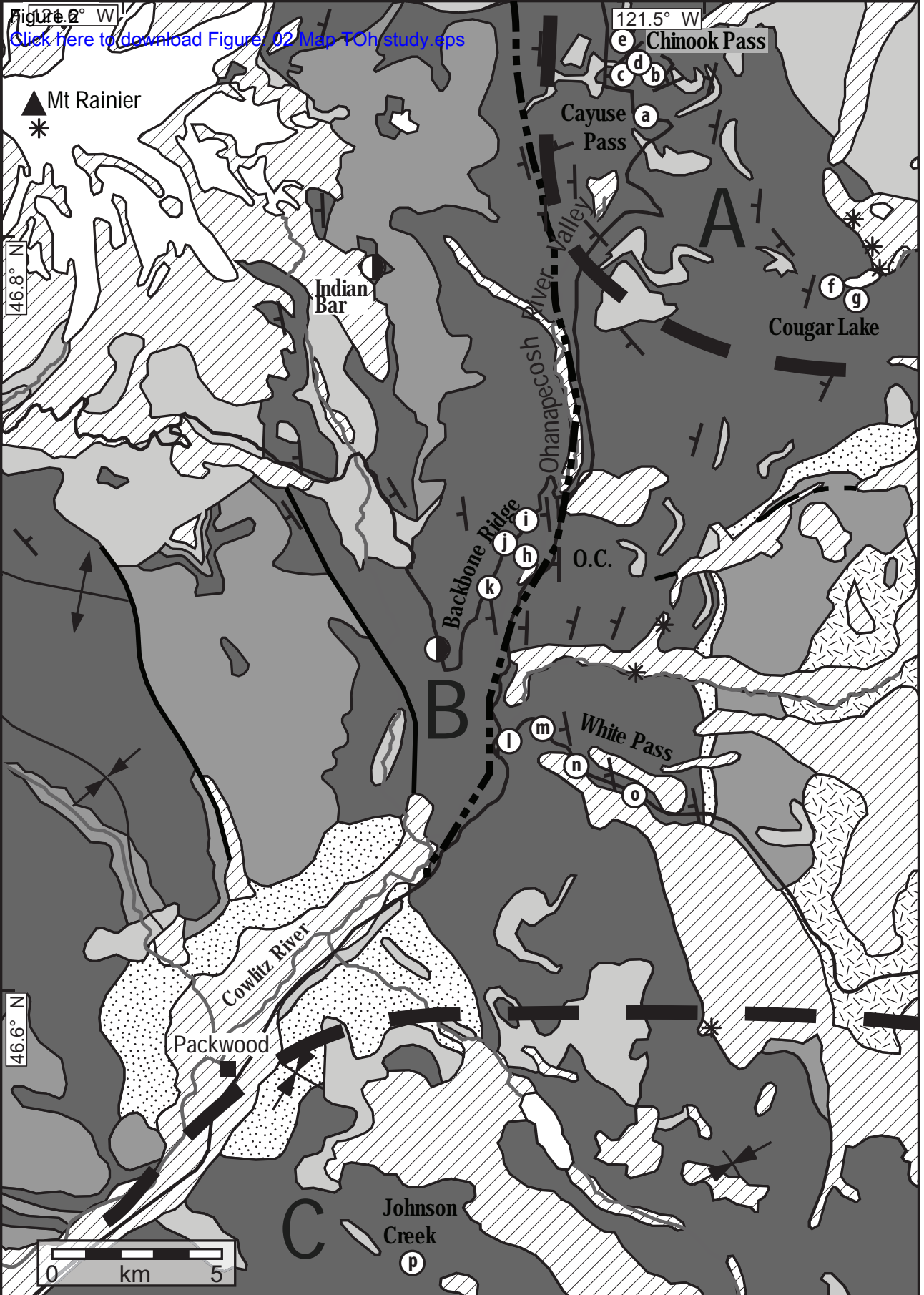
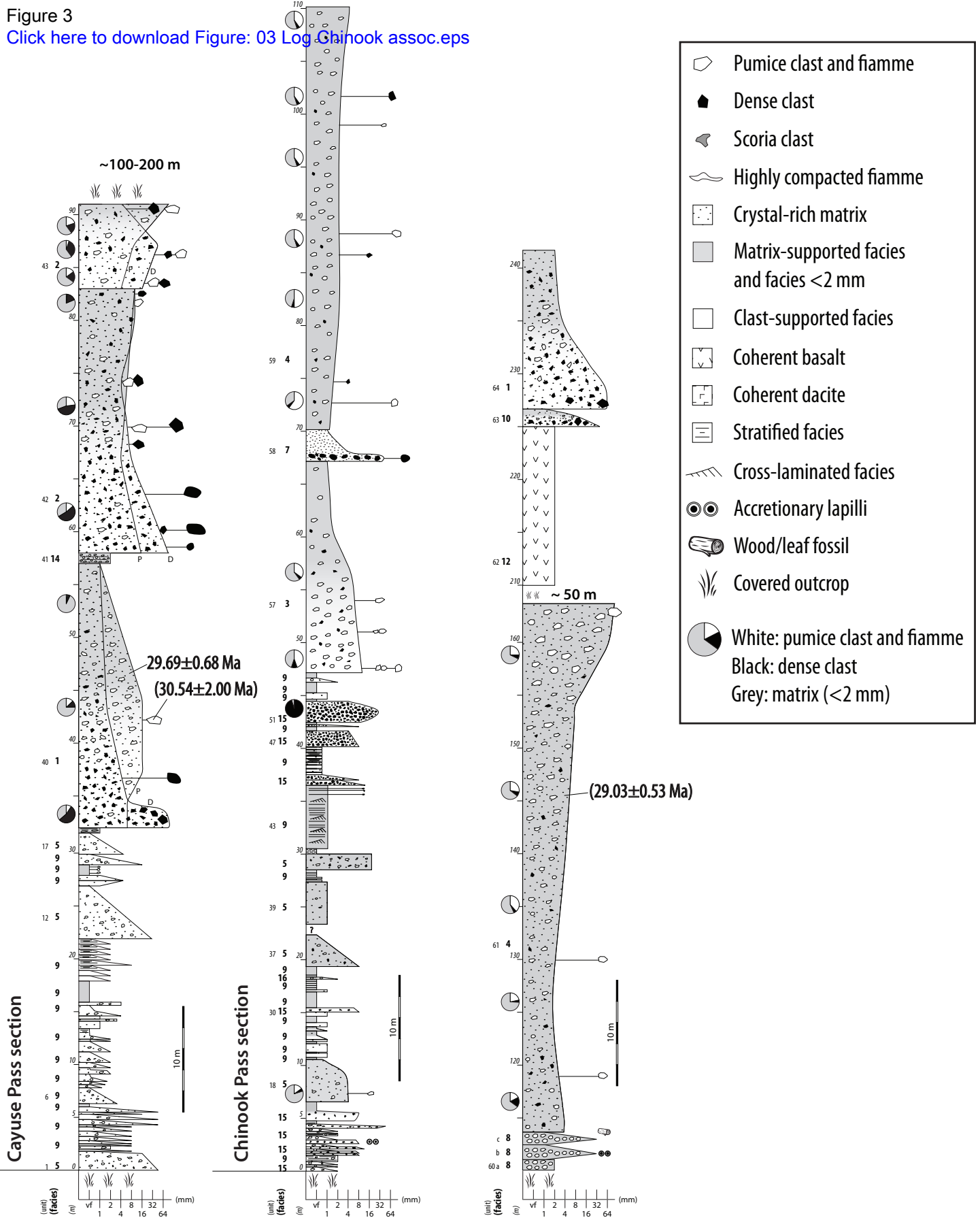


Figure 3
[Click here to download Figure: 03 Log_Chinook assoc.eps](#)



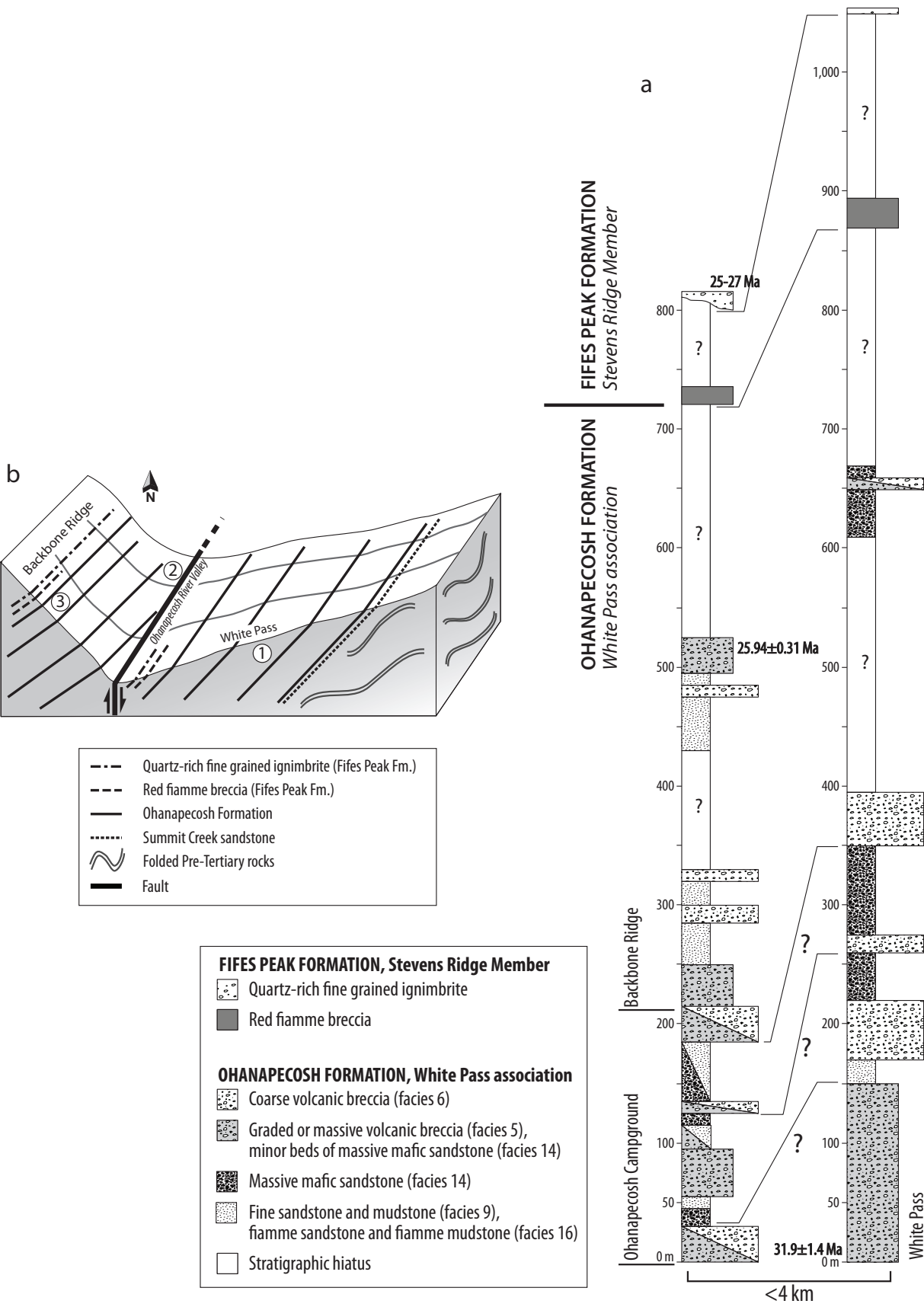
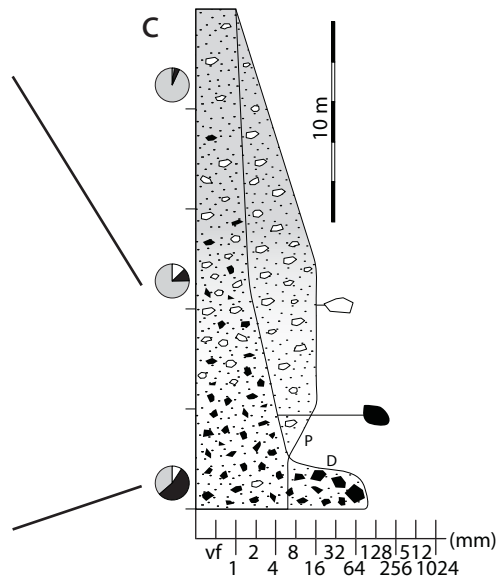
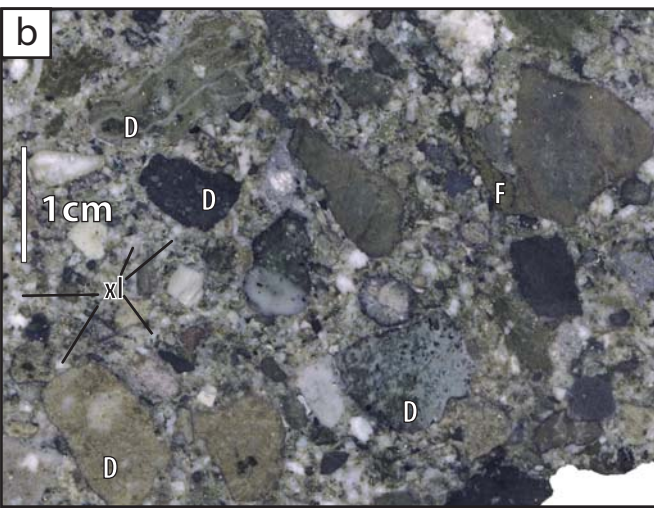
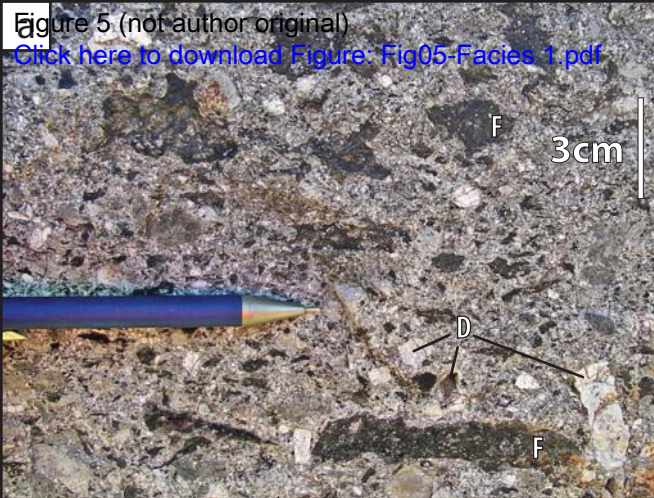


Figure 5 (not author original)

[Click here to download Figure: Fig05-Facies 1.pdf](#)



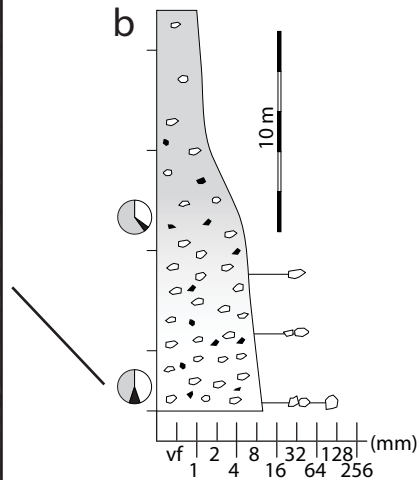


Figure 8 (not author original)
[Click here to download Figure: Fig08-Facies 4.pdf](#)

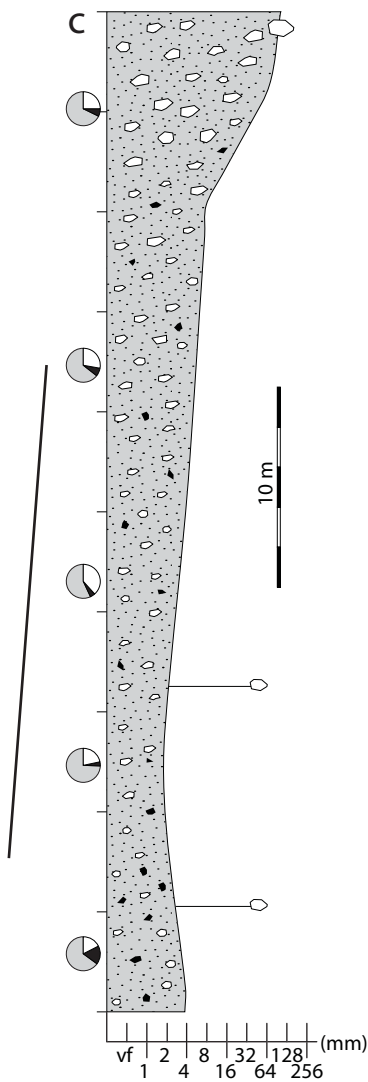
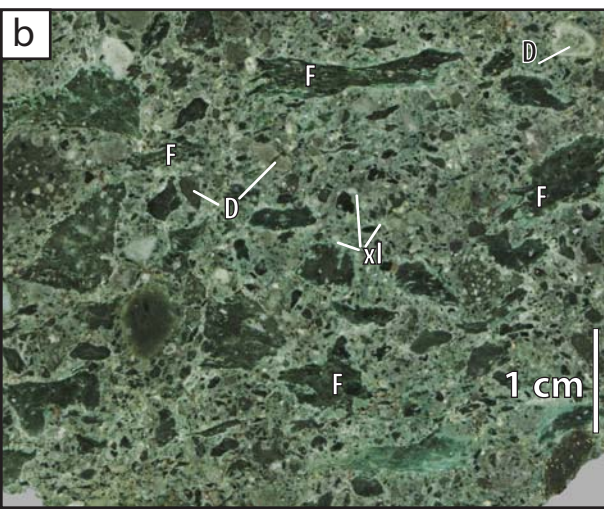
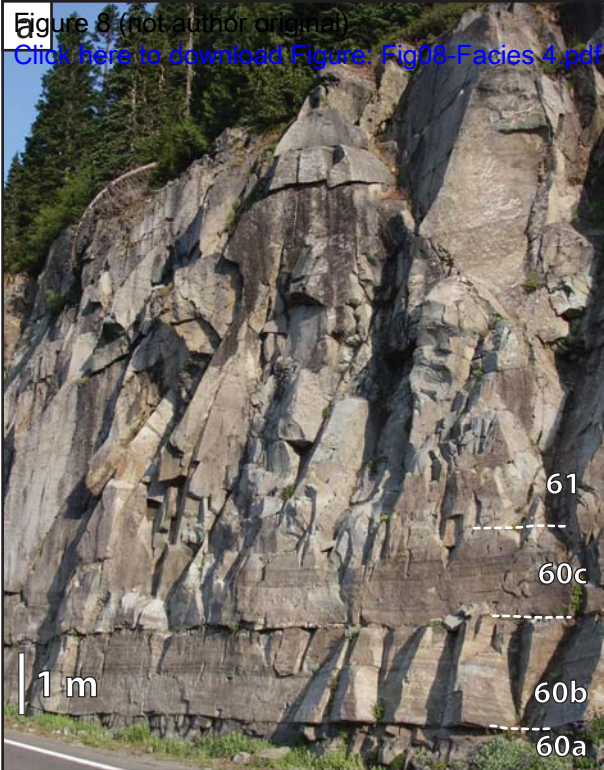
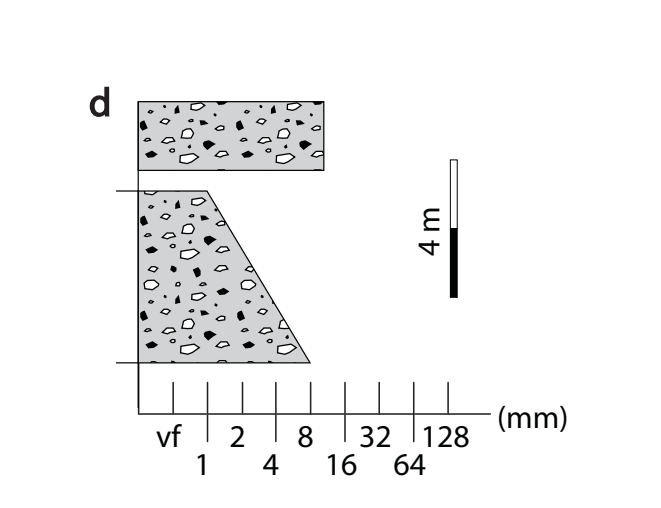
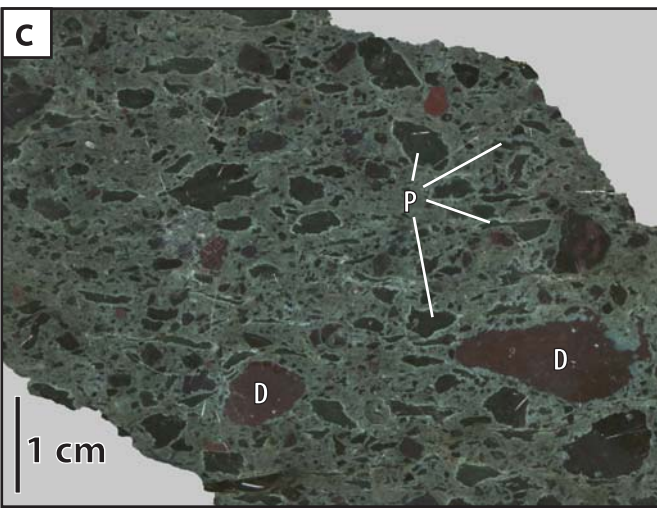
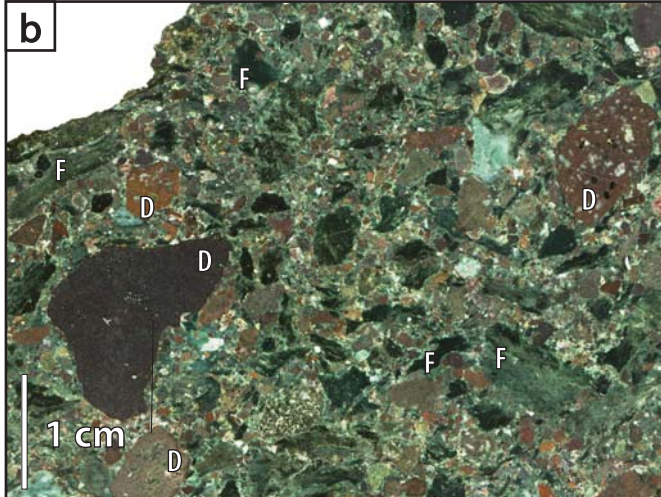
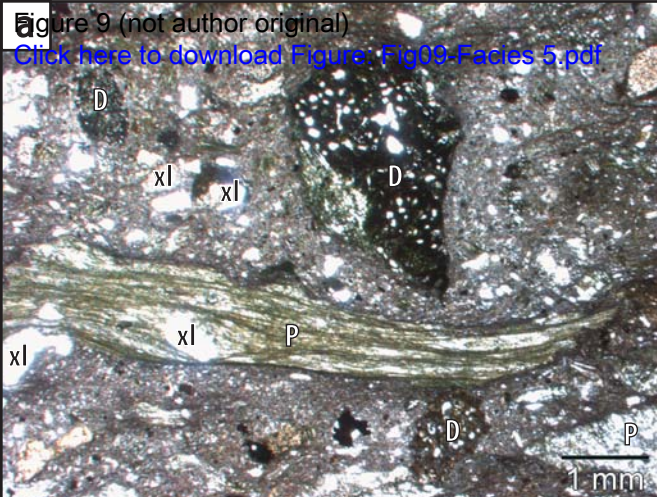
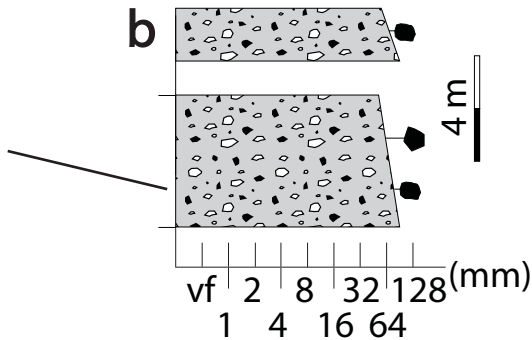
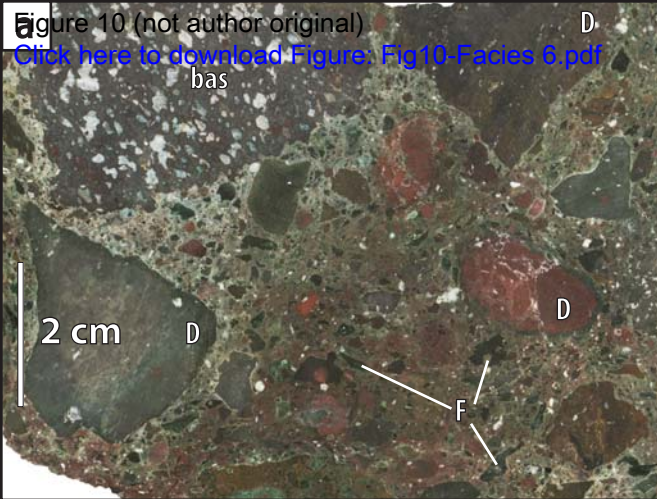


Figure 9 (not author original)

[Click here to download Figure: Fig09-Facies 5.pdf](#)





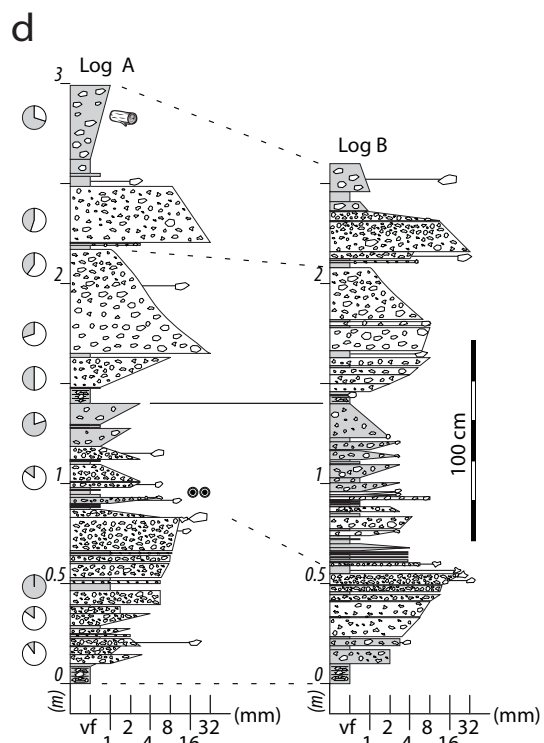
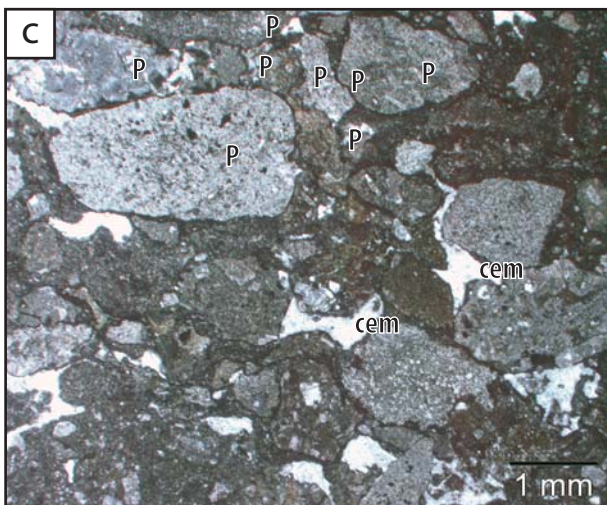
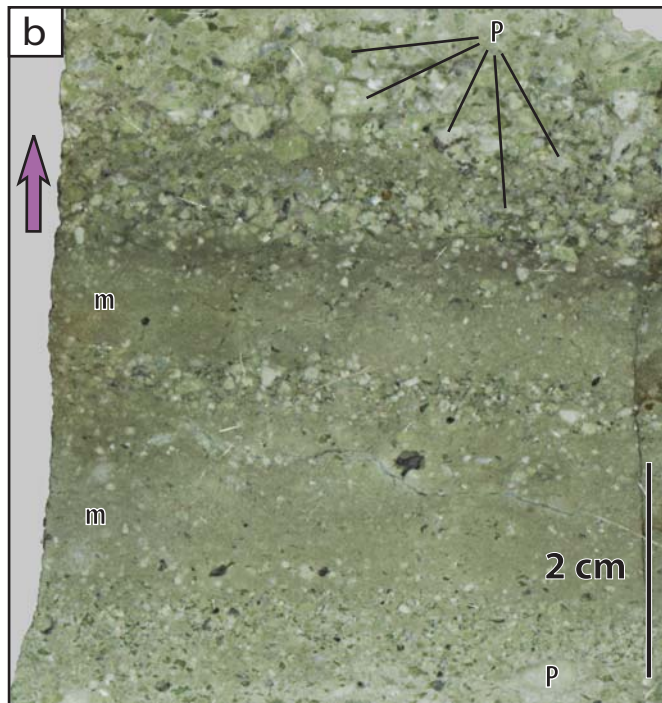


Figure 12 (not author original)

[Click here to download Figure: Fig12-Facies 9.pdf](#)

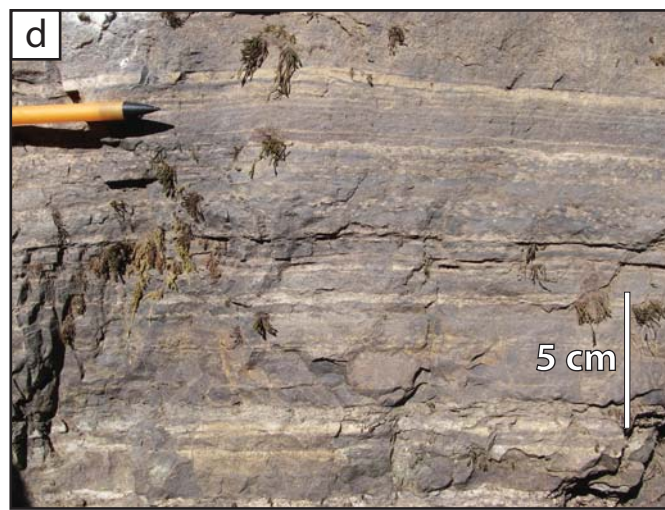
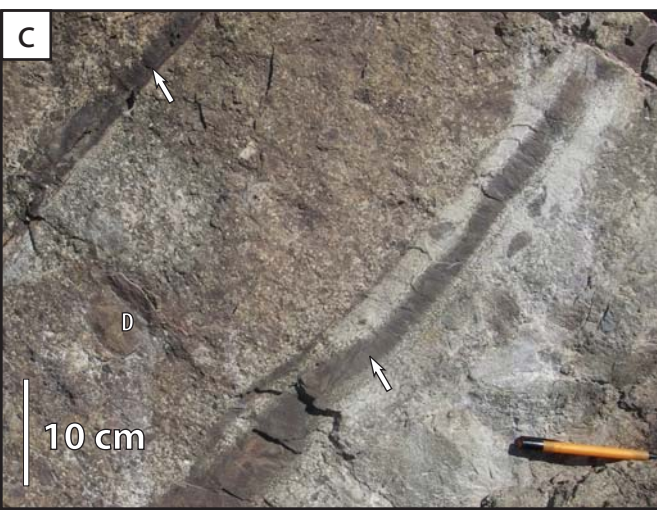
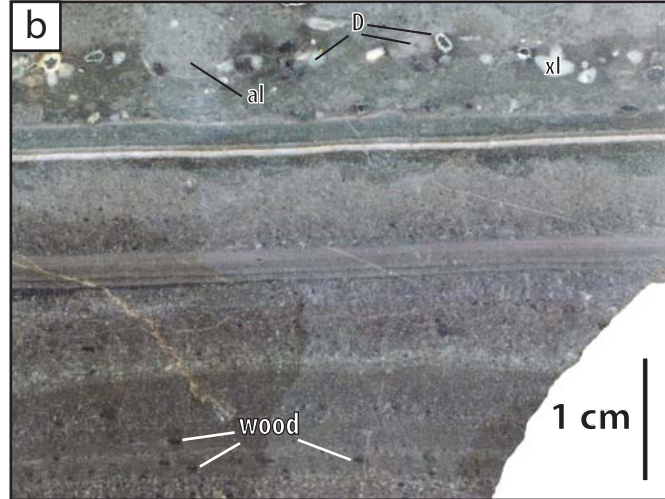
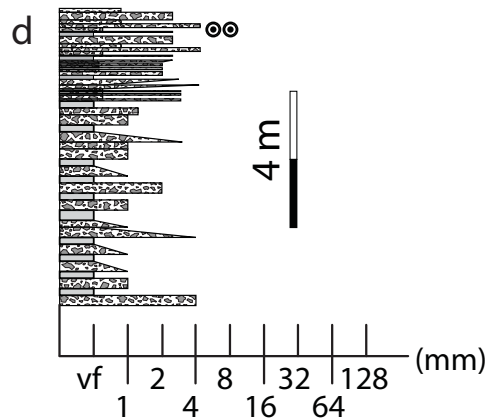
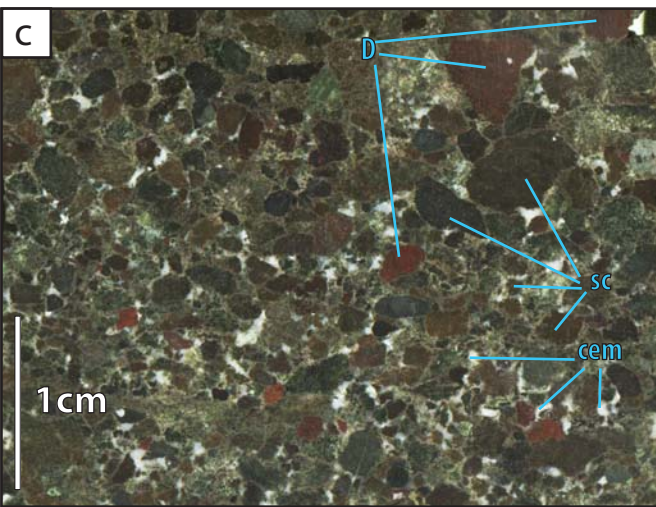
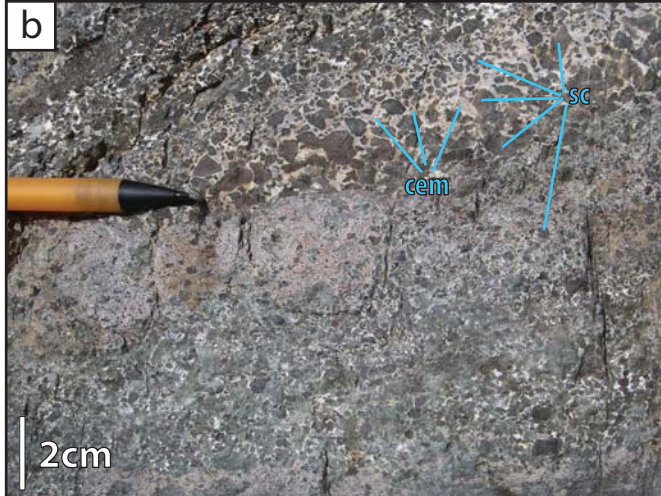
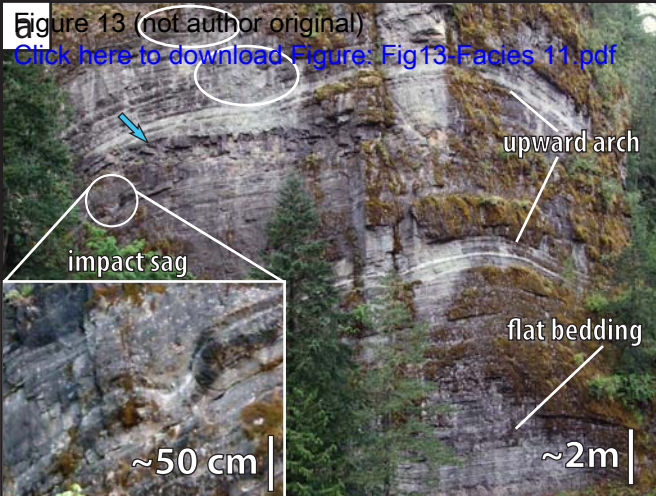
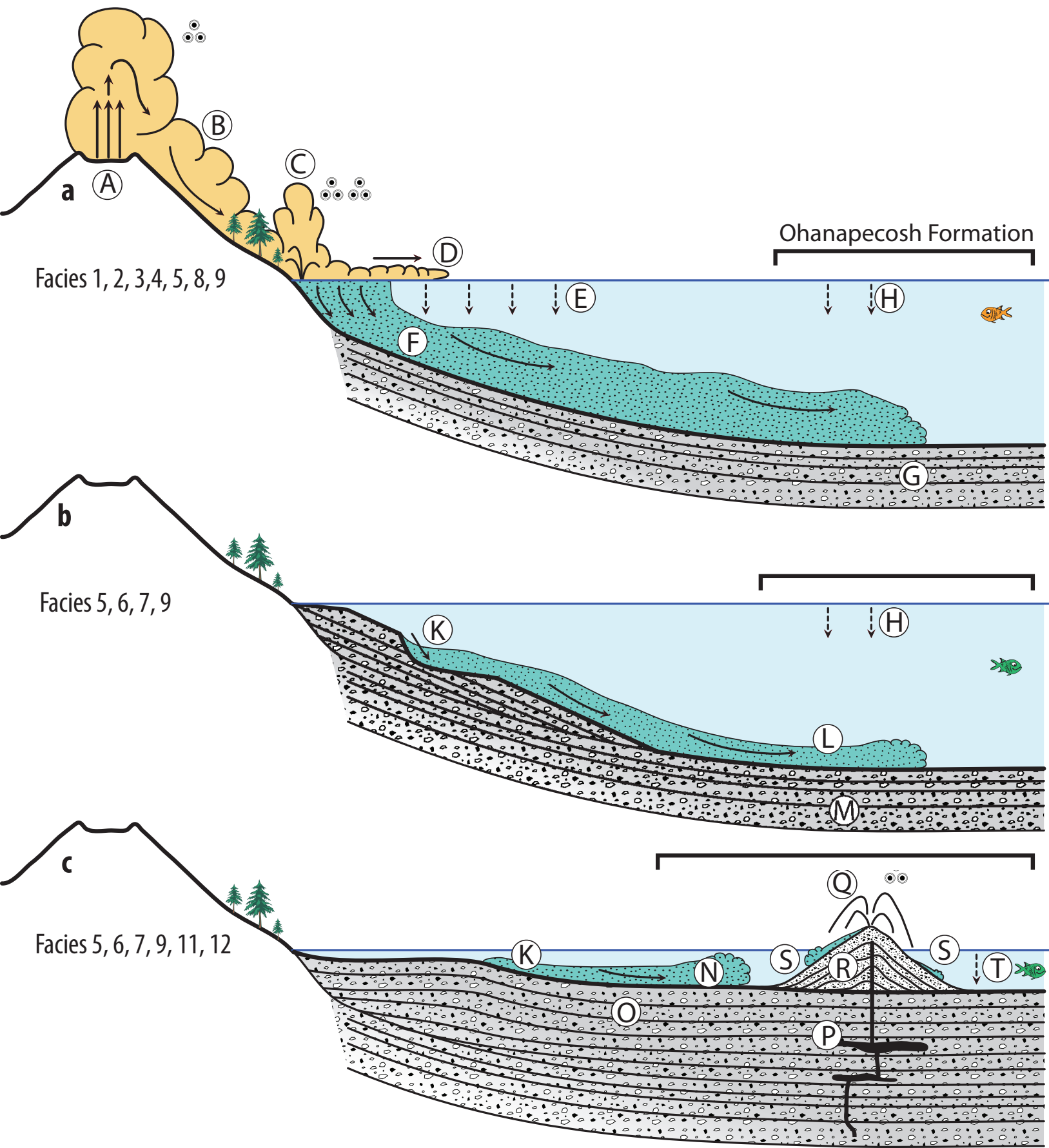


Figure 13 (not author original)

[Click here to download Figure: Fig13-Facies 11.pdf](#)





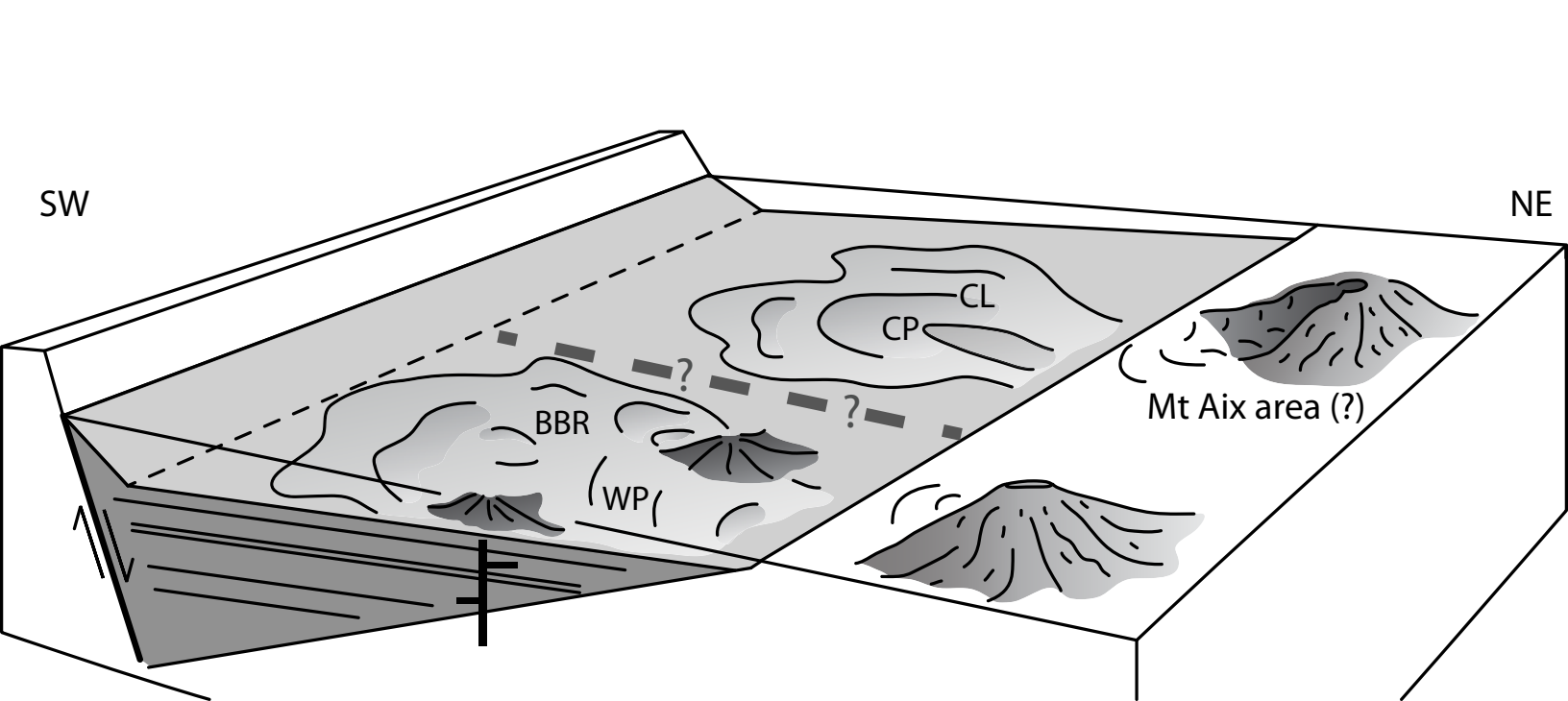


TABLE 1. CLASTS IN THE OHANAPECOSH FORMATION

Clast type	Color and size	Crystals	Other textures
Pumice and fiamme	1–60 mm; max 300 mm. Pale to dark green to black.	Largely euhedral phenocrysts, 0–20 vol.% in general. Plagioclase and mostly altered ferromagnesians; no quartz. Chinook Pass association: 25–30 vol.% phenocrysts (up to 5 mm) in coarse fiamme; small fiamme aphyric or too small to contain crystals. White Pass association: generally <30 vol.% phenocrysts.	Pumice clasts mostly angular. Former groundmass entirely devitrified, composed of secondary minerals. Aspect ratio of pumice clasts is 1–2.5 on average, maximum 5 for fiamme. Vesicles rarely preserved, round to very elongate (tube pumice, aspect ratio >>100).
Free broken crystals	N.A.	Mostly plagioclase; relics of ferromagnesians (pyroxene, amphibole). No quartz.	Broken on one face to multiple. Free crystal population matches the euhedral phenocryst populations in fiamme, pumice and dense clasts.
Scoria	2–10 mm. Red or dark grey to black.	Altered ferromagnesians common but difficult to distinguish from groundmass, feldspar microlites arranged in a trachytic texture, <1 vol.% plagioclase phenocrysts.	Sub-angular to very angular. Poorly to moderately vesicular (<40 vol.%), rounded to highly contorted vesicles (<0.1–1 mm across) filled with zeolites and other secondary minerals.
Accretionary lapilli	20 mm. Pale to dark gray, core up to 10 mm or absent.	N.A.	Rim-type accretionary and armored lapilli; commonly show multiple rims, and their cores are up to 10 mm (Cougar Lake, Ohanapecosh Campground) or absent (e.g. Backbone Ridge, Ohanapecosh Campground, White Pass). Broken and intact accretionary lapilli occur together.
Dense clasts	<1–1,000 mm. White Pass association: red, dark red, dark green, and dark brown dense clasts Chinook Pass association: white, green or dark green to dark brown aphyric dense clasts; lacks red dense clasts, except where in contact with Miocene Tatoosh sills.	0–50 vol. % plagioclase minor amounts of relic ferromagnesian crystals.	Range from rounded to very angular, but mostly angular.
Plant fossils	<1–20 mm. Black.	N.A.	Leaves, wood, rare >20 cm long silicified trunk fragment was found at lower Cayuse Pass.
Matrix	<2 mm. Pale to dark green, red to dark violet, braun to black.	Fragments of plagioclase crystals (0–15 vol.%) and relics of ferromagnesians.	Former groundmass entirely devitrified, composed of secondary minerals.

Note: N.A. = not applicable

TABLE 2. FACIES IN THE OHANAPECOSH FORMATION

Facies	Lithofacies	Typical unit/section; association	Unit thickness; grading	Clast and lithology
1	Normally graded fiamme-dense clast breccia	Cayuse 40, Chinook 64, Cougar Lake CPA	>15 m	Facies 1 is represented by unit 40 at Cayuse Pass, which consists of a >20-m-thick, tabular bed laterally continuous over >400 m (Fig. 5). It overlies a sequence of very thin to thick beds with a sharp contact (Fig. 3). Unit 64 at Chinook Pass is composed of similar facies, but less rich in pumice clasts and fiamme. It is exposed in a 15-m-high cliff (electronic suppl.) that overlies a thick (~1 m) bed of facies 10.
			Normal	base The basal sub-facies consists of 3 m of clast-supported, normally graded polymictic breccia, mostly composed of a variety of coarse dense angular to sub-rounded volcanic clasts (50 vol.%; some with all edges modified), dominated by dark aphyric dense clasts (Fig. 5). The size of the dense clasts gradually decreases upward from 60–80 mm to 6–10 mm, and rare sub-rounded oversized clasts occur (up to 1 m). The other components are abundant feldspar crystal fragments (>10 vol.% of the rock), black moderately porphyritic fiamme and pumice clasts (6–10 mm, 15 vol.%; 15–20 vol.% feldspar phenocrysts) and matrix (<20 vol.%).
				mid The middle sub-facies (10 m thick) is matrix-supported, normally graded breccia. The volume of dense clasts decreases to 10–15 vol.%, whereas fiamme become abundant (Fig. 5; >15 vol.%); average size is 10-20 mm and rarely up to 400x150 mm. The content of crystal fragments in the matrix remains high (>10 vol.%).
			top The upper sub-facies is normally graded, matrix-supported breccia (average diameter 6–2 mm, max 20 mm) and occupies the upper third (6–7 m) of the unit. Fiamme are minor (<5 vol.%) and the matrix is up to 90 vol.% and includes 20 vol.% of feldspar crystal fragments. At Cougar Lake, coarse tube pumice clasts (max 30 cm) occur in unit A1. Several m-long altered, tabular clasts (possibly stratified mudstone or coarse fiamme) are present at the top of unit B7. Poorly exposed, laminated or cross-laminated mudstone (>10 m thick) above may be part of the unit.	
2	Normally graded dense clast-fiamme breccia	Cayuse 42 CPA	>20 m	Facies 2 is >20 m thick, tabular and laterally continuous over >400 m. Directly overlies a 1-m-thick interval of laminated crystal-rich sandstone (facies 14) with a sharp boundary (Fig. 3). Very similar to facies 1, but rounded dense clasts are coarser and more abundant in this facies (Fig. 6).
			Normal	base The lower sub-facies is <10 m thick. The angular to sub-rounded dense volcanic clasts (dominated by a green aphyric type) are normally graded from 80 to 10 mm in average size and account for 40–60 vol.% (clast-supported). Oversized clasts (up to 1 m) are sub-rounded (Fig. 6), some with all edges modified. Fiamme (up to 15 mm) are relatively abundant (15–20 vol.%). The matrix includes feldspar crystal fragments and dense clasts.
				top The upper sub-facies is matrix-rich (up to 80 vol.%). Dense clasts (15 vol.%, up to 25 mm), angular pumice clasts (8–10 mm) and small fiamme (<5 vol.%; <4 mm) are also present.
3	Normally graded fiamme breccia	Chinook 57 Cougar Lake B10 CPA	>20 m	Facies 3 is poorly preserved, in tabular, 20-m-thick beds with two gradational sub-facies of similar thickness.
			Normal	base The basal sub-facies is clast-supported in pale-to-dark green fiamme and pumice clasts (Fig. 7; >40 vol.%, 10 mm average, max 30 mm), feldspar crystals fragments (5–10 vol.%) and minor sub-rounded dense clasts (<5 vol.%, up to 15 mm).

				top	The size and abundance of fiamme and pumice clast is smaller than in basal sub-facies (30 vol.%, 2-3 mm average), and this sub-facies is matrix-supported. The size of dense clasts is smaller and their abundance remains similar than the basal sub-facies.
4	Reversely graded fiamme breccia	Chinook 59, Chinook 61 CPA, (WPA)	>40 m Reverse	base	Facies 4 consists of tabular, 40- to 50-m-thick beds (Fig. 8). A bed at the top of Backbone Ridge (White Pass association) is tentatively included in this facies. The basal sub-facies contains pale-to-dark green fiamme and pumice clasts (40 vol.%, 2–5 mm), feldspar crystal fragments (>10 vol.%), dense clasts (<5 vol.%) and matrix. The fiamme and pumice clast sizes increase to 10 mm upwards (Fig. 8) and feldspar crystal fragments become more abundant (>15 vol.%).
				top	The upper 10 m of the unit shows a drastic increase in fiamme and pumice clast sizes (average 30-40 mm, max 150 mm). Less than 5 vol.% of dense clasts is found throughout the whole bed.
5	Graded or massive volcanic breccia	White Pass WPA, JCA, (CPA)	mostly 1–5 m, max 15 m Normal, massive; rarely reverse		This facies is made of very thick beds that can be clast-supported or matrix-supported, and dominated by fiamme or dense clasts (Fig. 9). The average grain size decreases from 10 to 4 mm upwards, or shows no change (10 mm). The components are green to dark grey fiamme and pumice clasts (Fig. 9; 30–60 vol.%), very angular dense clasts (10–30 vol.%), feldspar crystal fragments and matrix (20–60 vol.%). The dense clasts are a mixture of red- and dark-grey clasts of probable mafic and intermediate composition. Reversely graded units (southern Packwood, Johnson Creek association; top of the Backbone Ridge section) have similar characteristics except the increase in clast size.
6	Massive volcanic breccia	White Pass WPA, JCA	mostly 1–5 m, max 25 m Massive or normal		This facies occurs at White Pass, Ohanapecosh Campground and Backbone Ridge (White Pass association) and shows slight coarse-tail normal grading in the size of dense clasts (Fig. 10; 60 to 40 mm). Clasts are angular to sub-rounded. Dense clasts (50–70 vol.%), pumice clasts and fiamme (10–20 vol.%), and feldspar crystal fragments together are dominant over matrix (10–25 vol.%). Fiamme are green to dark grey.
7	Polymictic breccia-conglomerate	Chinook 58 CPA	3 m Normal		This facies separates two extremely thick beds of facies 3 and 4; it is poorly preserved. It contains abundant (>60 vol.%) sub-rounded to rounded, poorly porphyritic dense clasts (40 mm average, 200 mm max) at the base of the unit, and grades into fine-grained facies.

8	Reversely to normally graded pumice breccia	Chinook 60 CPA	2.5 m Reverse and normal	<p>Beds of this facies are laterally extensive over >100 m. The main part of the facies consists of pumice breccia chiefly composed of pale yellow to pale brown sub-rounded pumice clasts (average 1 to 10 mm, max 30 mm), with minor fiamme and rare feldspar crystals fragments (<1 mm) and <2 cm, unbroken and broken, rim-type accretionary lapilli (Fig. 11). The mudstone at the top of the units contains wood fragments (<2 cm). The grading of the pumice breccia is laterally continuous over tens of meters, but mudstone interlayers vary in thickness laterally and commonly disappear locally.</p> <p>Unit 60a is poorly preserved and its base is covered by vegetation. The base of unit 60b overlies unit 60a with 20 cm of smooth erosional relief over 3 m laterally. In units 60b and 60c, there are six main beds that are reversely to normally graded and range from clast-supported to matrix-supported (Fig. 11). Most units are interrupted with tens of laminae or very thin beds of mudstone. The upwards continuity in the reverse and normal grading of the pumice clasts in the pumice breccia is continuous, despite the intercalation of mudstone (Fig. 11). The matrix is made of pale yellow to pale brown mudstone of similar color to the sub-rounded pumice clasts. The mudstone matrix is absent in a few places and inter-clast space is filled with calcite and zeolite cement.</p>
9	Fine sandstone and mudstone	Ohanapecosh Formation CPA, WPA, JCA	1 mm – 1 m Massive or normal	<p>Laterally extensive, very thin to thick beds of fine sandstone and mudstone facies are present throughout the Ohanapecosh Formation (Fig. 12). The beds are laterally continuous and uniform in thickness; very rare cm-deep scours and cm-wavelength cross-laminations occur. The beds commonly occur in m-thick groups separating groups of very thick to extremely thick beds. Beds can be dark grey, purple or pale grey and most beds are probably composed exclusively of volcanic components. Crystal content is commonly <10 vol.%, but can reach >20 vol.%. Small pieces of wood (<1 cm) as well as rare accretionary lapilli and armored lapilli are spread throughout the thickness of some of the thin beds or concentrated in layers within very thin beds, especially in the Backbone Ridge section (White Pass association). Wood fragments are present in some beds; the largest fossil wood trunk was found in a pale grey unit at lower Cayuse Pass (Chinook Pass association). In the southern Packwood region (Johnson Creek association), fossil leaves are abundant in a >3-m-thick unit of cross-laminated fine feldspathic sandstone that was interpreted by Winters (1984) to have continental source.</p>
10	Normally graded dense clast breccia to fiamme breccia	Chinook 63, Cougar Lake CPA	1 m Normal	<p>The facies is clast-supported and consists of coarse dense clast breccia at the base (up to 40 cm thick), that grades upwards into fiamme breccia (fiamme 10–40 mm long); it is overlain by massive black sandstone to mudstone.</p>
11	Basaltic scoria breccia	White Pass 137 WPA	<1 m Normal	<p>This facies occurs in thin to thick, normally graded beds, and is composed of very angular scoria clasts (average 2-4 mm, max 10 mm). The scoria clasts are red to dark brown, and contain ovoid to highly contorted vesicles. The abundance of feldspar microlites is variable. The matrix makes up 20–95 vol.%, and the clast-supported varieties have monomodal grain size distribution and are cemented by white zeolites (Fig. 13).</p> <p>In a cliff close to White Pass (unit 137), the gently undulating beds occur in a 70-100-m-thick succession that is discordant to the regional strike. The orientation of beds in the section defines an upward arch (Fig. 13), defining a scoria cone structure. This succession includes scattered <2-m-long depressions in fine-breccia beds that contain 0.5-1 m clasts. The unit 137 is interbedded with a minor amount of beds of facies 9, and a couple of them show high concentration of accretionary lapilli.</p>

12	Vesicular basalt	White Pass CPA, WPA	0.3 m – 3 m	The basalt has sharp contacts and is conformable with bedding. Coherent vesicular basalt contains ellipsoidal vesicles (1-2 cm across) filled by secondary minerals (zeolites). In unit 62 at Chinook Pass, the size of vesicles increases upwards, and the vesicles occur in bands. Large tortuous cavities up to 10 cm long are common in the Cougar Lake section. No associated brecciated facies is present, except for one, poorly preserved outcrop at White Pass (unit 107) where basalt is overlain by mafic volcanic breccia.
13	Flow-banded dacite	Cougar Lake CPA	30 m	Feldspar crystals (>20 vol.%, <1 mm) and flow-banding in this coherent facies contrast with the typically massive Miocene Tatoosh sills. The vertical and horizontal extent of the dacite remains undetermined due to erosion and difficult access, but it is possibly up to 30 m thick and continuous over several hundred meters laterally; the top of the unit is inaccessible. It directly overlies facies 9 with a sharp contact. No flow-banded clasts that could have been derived from this dacite body were found in the Ohanapecohsh Formation.
14	Massive mafic sandstone	White Pass WPA	<1 m Massive	Beds of relatively well-sorted, massive mafic sandstone mostly consists of red-oxidized to dark grey, poorly vesicular scoria clasts (>95 vol.%) of probable mafic composition and feldspar crystal fragments (<2 vol.%); fiamme are absent. The cement is composed of zeolites and other secondary minerals. The scoria clasts are made of minor feldspar laths and ferromagnesian phases. The vesicles are ovoid to highly contorted.
15	Fine, dense clast volcanic breccia	Chinook 51 CPA	10 cm – 2 m Normal, or reverse to normal	This facies is normally graded breccia dominated by pale grey, grey and black dense clasts; rare fiamme of similar size are also present. Clast size averages 8-10 mm; largest clasts are 25 mm across. The pale grey clasts contain minor feldspar crystals (<10 vol.%). The proportions of matrix and clasts vary from unit to unit, but dense clasts are commonly >60 vol.%.
16	Normally or reversely graded fiamme mudstone	Cougar B13 CPA, WPA	<1 m Normal or reverse	Normally or reversely graded fiamme mudstone is matrix supported. The average fiamme size is 2–4 mm; coarser fiamme (up to 50 mm) are minor. Rare cross laminae, dense clasts and wood occur.

Note: CPA, Chinook Pass association; WPA, White Pass association; JCA, Johnson Creek association.

TABLE 3. INTERPRETATION OF THE OHANAPECOSH FORMATION

Facies	Lithofacies characteristics	Transport process	Current behaviour	Eruption-fed versus resedimented products	Environment at source
1, 2, 3, 4, 5	Extremely thick (>20 m), laterally continuous beds, overall matrix-supported. Commonly dominated by angular pumice clasts; rich in crystal fragments. Facies 1, 2 and 3 have a basal dense clast breccia that is dominated by angular to sub-rounded dense clasts. Facies 5 spans from matrix- to clast-supported (20-60 vol.% matrix).	High-concentration density current, weakly cohesive	Non-cohesive current, deposited under some degree of turbulence. Sub-rounded coarse dense clasts in basal breccia suggest accidental pick-up. Reverse grading in facies 4 probably explained by lower density of larger pumice clasts present in the upper part of the bed, or delayed waterlogging.	Extreme thickness, abundance of angular pumice clasts and crystal fragments suggest products from explosive eruptions, fed directly from voluminous pumice-rich density currents.	Presence of facies 7 and 8, wood and accretionary lapilli in the beds of the Chinook Pass association suggests the entire sequence to be mostly derived from subaerial environment. Basal breccia composed of sub-rounded dense clasts suggests resedimentation of clasts abraded in above wave-base environment. Angularity of pumice clasts denotes short subaerial transport.
5, 6	Extremely thick (>20 m), laterally continuous beds that span from matrix- to clast-supported beds (20-60 vol.% matrix), and dominated by pumice clasts and fiamme or dense clasts. Rich in crystal fragments. Normally graded or massive, absence of basal dense clast breccia.	High-concentration density current, moderately cohesive	Absence of dense clast breccia and weak grading suggest a more coherent current behaviour. Sub-rounded coarse clasts in facies 6 indicate weak clast abrasion during transport, or accidental pick-up.	Very thick to extremely thick beds, and abundance of angular pumice clasts and crystal fragments suggest products from explosive eruptions or resedimentation. If eruption-fed, directly fed from voluminous pumice-rich density currents. If resedimented, pumice clasts were previously saturated (e.g. Allen and Freundt, 2006).	Where preserved, angularity of pumice clasts denotes short subaerial transport. Sub-rounded dense clasts suggests at least partial source from above wave-base environment. Presence of wood and accretionary lapilli in other beds of the White Pass association suggests that part of the sequence is derived from subaerial environment.
7	Very thick, normally graded breccia-conglomerate that is dominated by sub-rounded to rounded dense clasts at its base. Pumice clasts and fiamme absent.	High-concentration density current	Strong normal grading in relative thin bed indicates weakly cohesive current.	Relative small thickness and absence of pumice clasts and fiamme suggests deposition from a density current.	Resedimentation of dense clasts previously abraded in above wave-base environment.

8	<p>Thick, laterally continuous, reversely to normally graded, well sorted beds. Dominated by sub-rounded pumice clasts and former glass shards. Numerous very thin mudstone interbeds composed of presumed former glass shards do not interrupt grading in pumice clasts. Accretionary lapilli and wood are present in few mudstone interbeds.</p>	Vertical settling	<p>Distinctive reverse grading and presence of sub-rounded pumice clasts records saturation grading from progressive waterlogging of pumice clasts as a function of their size. Beds with normal grading indicate that the coarsest particles sank faster than the smaller ones, in a type of sedimentation dominated by hydraulic sorting. Interbeds of former glass shards reflect complex sedimentation of fine-grained clasts contemporaneously with the sinking of the pumice clasts. Origins could be abrasion of pumice clasts that formed the raft, ash from disintegration of pyroclastic flows at the shoreline, or fallout of ash from atmospheric ash plumes.</p>	<p>Eruption-fed, and formed in a two-step process: (1) a pumice-forming subaerial explosive eruption deposited pumice lapilli and ash onto the water body, forming pumice rafts (e.g. White et al., 2001), and (2) subsequent waterlogging in pumice rafts and settling of the pumice clasts, ash, wood and accretionary lapilli.</p>	<p>The accretionary lapilli demonstrate the presence of wet, ash-rich clouds (Cas and Wright, 1991); wood indicates source to be at least partially subaerial. The formation of pumice rafts is likely to be associated with deposition of pumice clasts that cooled in the atmosphere (Whitham and Cas, 1991).</p>
9	<p>Relatively thin (<1 m), laterally continuous, normally graded to massive beds. Contains mostly fine-grained (<2 mm) components. Wood, pumice clasts and accretionary lapilli can occur in small amount.</p>	Low density density current; vertical settling	<p>Good grading and fine-grained nature of the beds indicate deposition from low density currents or vertical settling processes.</p>	<p>Vertical settling of explosive eruption-fed products or resedimentation of saturated unconsolidated aggregates.</p>	<p>Subaerial eruption plumes deposited onto water, or resedimentation of unconsolidated aggregate.</p>
11	<p>Normally graded, laterally continuous, clast-supported and dominated by angular scoria clasts and crystal fragments, interbedded with beds of fine sandstone and mudstone (facies 9) that rarely contain accretionary lapilli. Unit 137 in White Pass section shows a scoria cone architecture with impact sags, and is associated with vesicular basaltic intrusions (facies 12). Dip and strike differ from general structure of the Ohanapecosh Formation.</p>	Grain flow, low density density current; vertical settling	<p>Normal grading, and clast-supported facies indicate deposition from overall non-cohesive, dilute density current, vertical settling or grain flow.</p>	<p>Scoria cone, impact sags, accretionary lapilli in mudstone interbeds and scoria-clasts-dominated deposits suggest eruption-fed facies, such as surtseyan. However, slopes on scoria cones are typically unstable and partial resedimentation of loose aggregates over a short distance is probable.</p>	<p>Scoria cone, impact sags and accretionary lapilli indicate subaerial or shallow-water (<30 m) vent environment. Different dips and strikes with other beds of Ohanapecosh Formation denote this facies to be localized and intrabasinal.</p>
